NTNU
Norwegian University of Science and Technology

The Effect of mechanical mixing and Porosity on the Activity of Ag and Cu Ion exchanged Zeotypes in the HC-SCR of NOx with Propene

Georg Botne

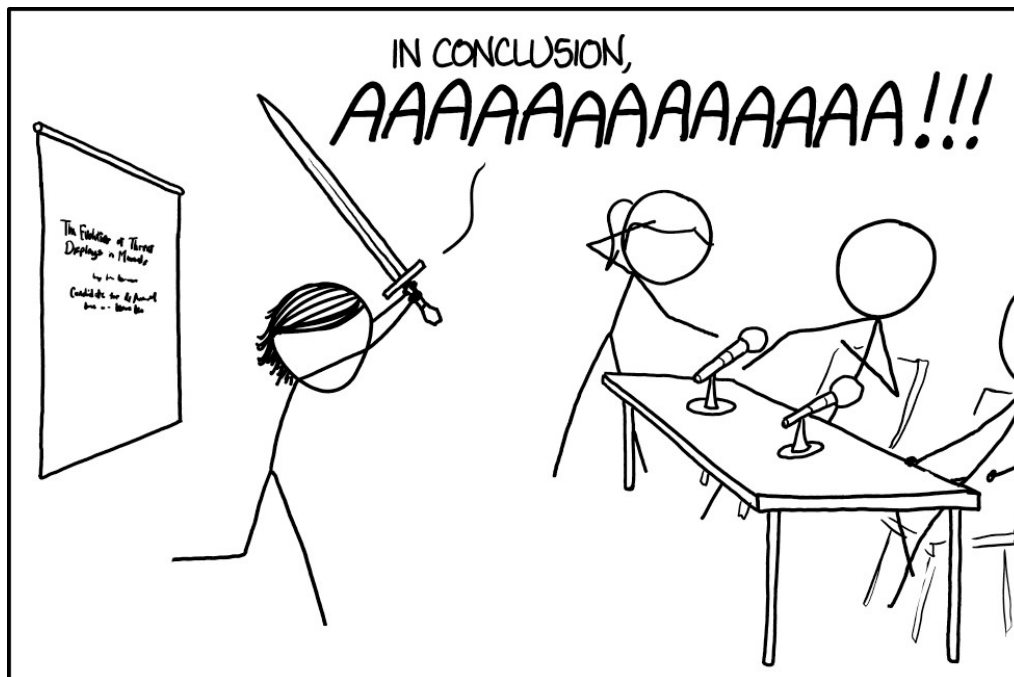Master of Science
Submission date: December 2017
Supervisor: Karina Mathisen, IKJ

Norwegian University of Science and Technology
Department of Chemistry

The effect of mechanical mixing and porosity on the activity of Ag and Cu ion exchanged zeotypes in the HC-SCR of NO_x with propene

Georg Botne

Master Thesis

THE BEST THESIS DEFENSE IS A GOOD THESIS OFFENSE.

"If you visit American city

You will find it very pretty

Just two things of which you must beware:

Don't drink the water and don't breathe the air!"

-Tom Lehrer, Pollution.

Acknowledgements

Firstly, I would like to thank my supervisor, Dr. Karina Mathisen, and Ph. D. candidate Guro Sørli. I wouldn't have been able to do this on my own, and I have greatly appreciated your unending support, advice and feedback. Thank you for pushing me and providing your valuable insight; it has inspired me to give it my all. Thank you for guiding me through this with humour and friendship; it made it all the better.

My gratitude also goes to all the silly and helpful people in the lab; Karsten, Daniel, Stian, Caren, Simon, Tengzhi, Anders H, Gaute, Anders G and Sigurd. It wouldn't have been nearly as fun to work in the lab without you lovely people. I value your support and strangely good music.

Finally, I must thank Ellen Marie. Thank you for soothing my worries and insisting it will all be fine. Somehow, you were right!

Abstract

The effect of mechanical mixing and porosity of Ag and Cu ion exchanged zeotypes in the hydrocarbon selective catalytic reduction (HC-SCR) of NO_x with propene has been investigated. To this effect, mordenite, ZSM-5, and conventional and hierarchical SAPO-34 have been ion exchanged with Ag, Cu, or both simultaneously. Mechanically mixed samples have been prepared using equal parts Ag and Cu zeotypes. The crystallinity of the resulting samples has been verified by XRD, and the metal content has been determined by ICP-MS. The NO_x conversion has been measured by a chemiluminescence NO_x analyser.

It has been found that mechanical mixing causes reduced $deNO_x$ activity compared to Cu ion exchanged zeotypes. For simultaneously ion exchanged zeotypes with Ag and Cu, a synergistic effect is seen with smaller pore sizes. Physical separation and diffusion between crystallites is thought to cause the difference between simultaneously ion exchanged and mechanically mixed samples. Moreover, a peak $deNO_x$ conversion of 83% has been achieved with simultaneously ion exchanged conventional SAPO-34 at 425°C. This is attributed to differences in local coordination between the simultaneously ion exchanged sample and the mechanically mixed sample. Simultaneous ion exchange is seen to give increased total metal loading compared to Ag and Cu ion exchanged zeotypes.

Table of contents

Abbreviations

- [Ag+Cu]:Z – Mechanically mixed zeotype with Ag and Cu
- AgCu:Z – Simultaneously ion exchanged zeotype with Ag and Cu
- CHA – Framework type
- $DeNO_x$ – The conversion of NO_x
- EEA – European Environmental Agency
- FER – Framework type
- GCMS – Gas chromatography–mass spectrometry
- HC – Hydrocarbon
- HC-SCR – Selective catalytic reduction with hydrocarbons
- ICP-MS – Inductively coupled plasma – Mass spectrometry
- Me:Z – Ion exchanged zeotype with metal
- MFI – Framework type
- MOR – Framework type
- NO_x – NO and NO_2
- Ppm – Parts per million by volume
- SCR – Selective catalytic reduction
- SSZ-15 – Mesoporous silica
- WHSV – Weight hourly space velocity
- Wt% – Weight percent
- XRD – X-ray diffraction

1.0   Goal of the thesis

Air pollution is a continuing challenge of the industrialized world. The toxic smog in Delhi, India in November 2017 exemplify the lack of good solutions to improve local air quality.[5] Emissions of automotive vehicles are thought to be a considerable part of the problem. These emissions contain gases like hydrocarbons, carbon monoxide and NO_x which are released upon the burning of fossil fuels.

In lean burn engines, where a high oxygen content is used, the emissions of NO_x gases are particularly high. As of today, no good catalyst exists for the reduction of NO_x into N_2 in lean urn engines. The goal of this thesis is to find candidates for better and cheaper NO_x reduction in small vehicles, which may significantly reduce local air pollution. To this end, zeolite supported transition metals are often used. Pt is currently researched for HC-SCR, but is expensive.[6] By comparison, Cu is active for selective NO_x reduction with hydrocarbons at higher temperature, and the price of unalloyed Cu in 2015 was \$6.3/kg on average, vastly lower than the Pt average of \$36000/kg.[6] Likewise, Ag has been used for HC-SCR, and its average price was \$400/kg in 2015.[6-8]

Although no single catalyst currently satisfies the needs for NO_x reduction, mechanically mixing two catalysts with different metals is a potential solution which has received little attention.[3, 9-10] If mechanical mixing of two metal containing zeotypes yields a catalyst with mixed properties, mixing could be a potential method for creating catalysts with desired properties. It is however not well known which effect, if any, mixing two metal containing zeotypes has, and to which extent zeotype porosity influences the mixed catalyst. Therefore, the effect of mechanical mixing and porosity of Ag and Cu containing zeotypes on the HC-SCR of NO_x is investigated in order to determine the potential of the method for making effective low-cost catalysts for the future.

2.0   Introduction

As part of an international effort to improve air quality, reducing pollution from road traffic is vital. In Norway, road traffic is the most important source of local air pollution.[11] In this regard, a transition to electric and zero emission vehicles is seen as a solution. Despite the emergence of electric vehicles and similar technologies, current research suggests that this transition to an electric car fleet is greatly dependent on external conditions like policy and cost efficiency.[12-13] Based on a model, Kihm and Trommer [14] suggest that one third of the annual mileage will be travelled by electric vehicles by 2030 in Germany. The study also finds that diesel cars are expected to be replaced later than petrol cars; gaining traction only after 2025.[14] Therefore, the aim to reduce emissions from fossil fuel vehicles is still highly relevant.

One possibility is to improve the current catalysts for exhaust clean-up. Stoichiometric fuel engines, which add the minimum oxygen necessary to complete the combustion reaction of fuel, have been used for a long time and have effective catalysts.[15-16] In this scheme, 14.7 parts oxygen by mass of fuel is used.[16-17] Under lean-burn conditions, however, where the oxygen concentration exceeds this amount, fuel consumption is notably lower.[9, 16] Although economically positive for the consumer, operating under lean conditions release more NO_x into the atmosphere.[18]

NO_x, comprised of NO and NO_2, is not only harmful to humans, but also to the environment in that it may both cause photochemical smog and acidify lakes and forests.[2, 19-21] As a result, ever more stringent automotive emission restrictions are put in place. This can be seen in the Kyoto Protocol, which aims to control and reduce the emission of several greenhouse gases.[22-23] Similar efforts are seen made by the European Environment Agency (EEA), where the Euro-standards for vehicles exemplify progressively tighter standards on automotive emissions.[24]

Several solutions for reducing NO_x emissions have been proposed, though not all are equally relevant for automotive vehicles. For instance, Selective Catalytic Reduction (SCR) is one class of reactions which aims to selectively reduce NO_x to N_2 by catalysis.[25] One method is called ammonium-SCR, and is currently employed in stationary chemical facilities and larger vehicles with ammonium or urea.[25] In this method, urea solution is added to the system post-burn of the fuel, which reduces NO_x to N_2.[26] In passenger cars, however, the use of an additional fuel tank appears highly impractical, and may even increase other emissions due to the extra weight. It

would also increase the risk of chemical spills of urea and necessitate additional widespread transport of chemicals.

A second method, simultaneously proposed by two separate research groups in 1990, aims to use excess hydrocarbons in vehicle exhaust to reduce NO_x to N_2.[27-29] Named hydrocarbon-SCR (HC-SCR), this is a more practical approach for smaller vehicles, as it would not necessitate further addition of chemicals than what already exists.[29] To this extent, some headway has been made with zeotype supported transition metals; a vastly increased catalytic activity and specificity can be achieved.[3, 30-31] Platinum has been used, but is expensive and suffers from unwanted production of N_2O.[3] To replace platinum, copper and silver are cheap alternatives. Zeotypes with ion exchanged copper show great promise in the conversion of NO_x, though the activities of many copper containing zeotypes are reduced strongly with the introduction of water or SO_2.[7, 30-31] Silver has also shown to be active in HC-SCR, and though it is less active than copper, it is considerably more hydrothermally stable when ion exchanged into zeotypes compared to copper zeotypes.[7]

Though catalytic results are improving; few single materials seem to satisfy the complete needs of NO_x catalysis. One proposed method, however, uses the mechanical mixing of ion exchanged zeotypes with different properties and porosity, thereby attempting to find a satisfactory combined catalyst.[10] Ideally, a mechanically mixed catalyst will combine the properties of its components, and thereby yield a satisfactory $deNO_x$ catalyst. This idea, though expressed as early as 2000, has seen little investigation.[9-10, 32] Furthermore, though ion exchange is a common method to incorporate metals into zeotypes, the effect of simultaneously ion exchanging two metals has barely been considered.

Given the above discussion, this master's thesis aims to investigate the effect of mechanical mixing and porosity on the $deNO_x$ activities of Ag and Cu ion exchanged zeotypes. To achieve this, each zeotype will be ion exchanged with Ag, Cu, or both metals simultaneously. In order to determine the effect of porosity, the small pore zeotype conventional SAPO-34, medium pore ZSM-5 and large pore mordenite will be considered, along with the mesoporous hierarchical SAPO-34. The metal content will be verified by ICP-MS, and the degree of crystallinity will be verified by powder XRD. Furthermore, Ag and Cu ion exchanged zeotypes will be mechanically mixed. These samples will thereby be compared in the HC-SCR of NO_x with propene.

3.0   Theory

This section looks closer at what challenges are posed by NO_x and the structure and properties of zeolites and zeotypes, before moving on to selective catalytic reduction with hydrocarbons. Then, theory on metal loaded zeotypes in the reduction of NO_x is considered before presenting theory on XRD and ICP-MS.

3.1 The sources and challenges of NO_x

The emission of NO_x has notable negative effects on the environment, but also for humans.[2, 11] In this section, the sources of NO_x emissions are examined. This includes the mechanism of NO_x generation. Some implications of NO_x emissions are also considered, with focus on human health. Notably, the connection between NO_x and O_3 emissions is explored.

3.1.1 Sources of NO$_x$

The sources of NO$_x$ are both manmade and natural. NO$_x$ is generated in high temperature reactions with air, which are present during lightning.[19] In Norway, the manmade NO$_x$ emissions have steadily decreased in recent years as shown in Figure 3-1. The main source of NO$_x$ in 2016 was oil and gas extraction with 45000 tons or 43% of the total emissions. Road traffic is responsible for 29000 tons or 28% of the total NO$_x$ emissions. This is after a considerable decline in the emissions of aviation, aquaculture and maritime transport.
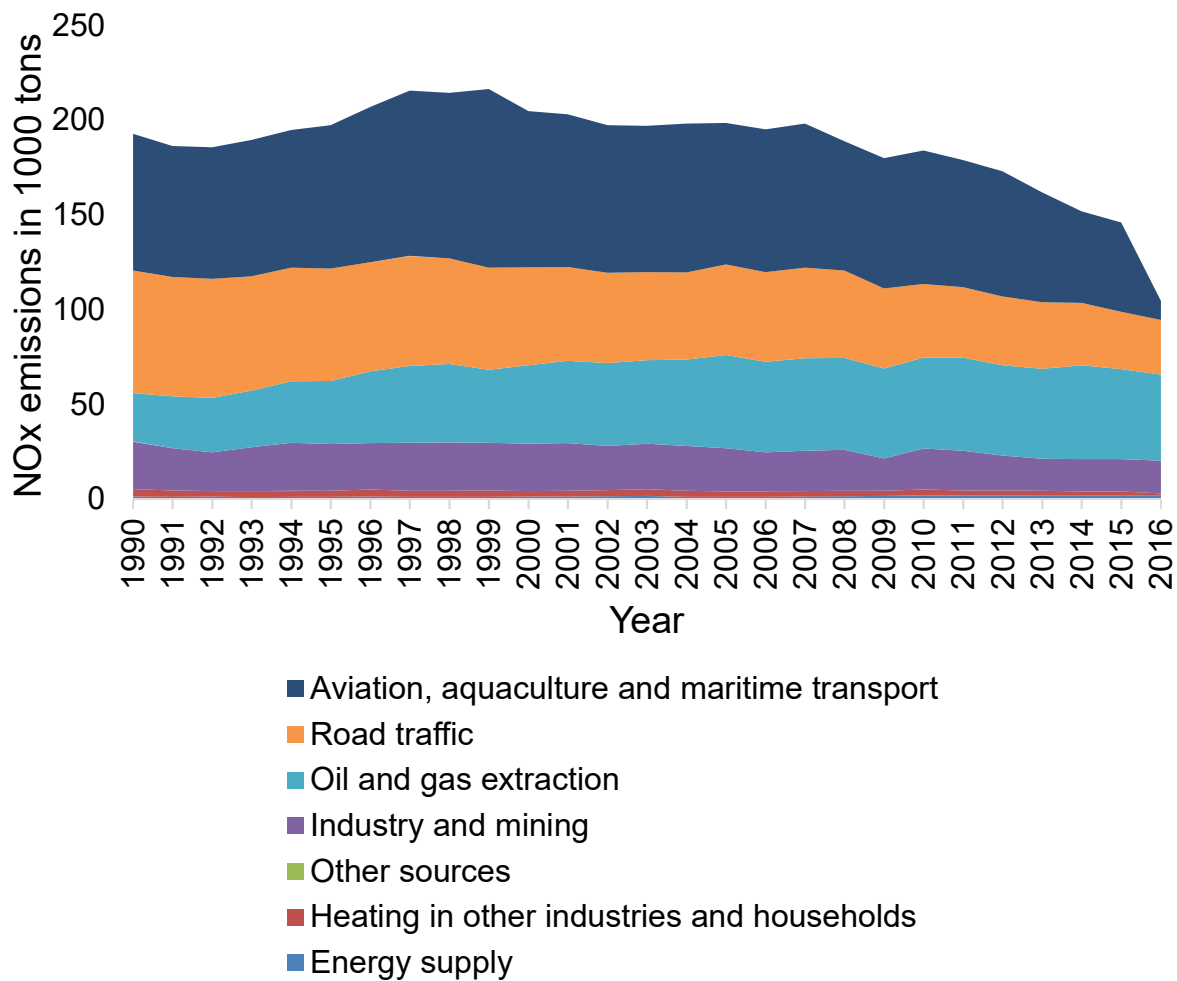
Figure 3-1: NO$_x$ emissions in Norway by source from 1990 to 2016.[2]

In the EU, the situation is different. Results published by the EEA with data from 2015, show that the largest contributor to NO_x emissions was road transport, totalling 38% of all manmade NO_x emissions.[33] As a result, reducing automotive NO_x emissions can be said to be the most potent way to reduce overall NO_x emissions.

Road transport is a major factor for several reasons. Firstly, whereas the original three-way catalyst worked well under stoichiometric conditions; this is less the case with the increased oxygen in lean-burn conditions which is typically used in diesel cars. Here, the reduction of NO_x gases has proven more difficult.[9] Lean burn engines also function at higher temperatures, leading to additional NO_x generation.[34] Furthermore, though it was already known that diesel cars release more NO_x gases than petrol cars; there seems to be a further discrepancy between the average measured NO_x release and tested NO_x release for diesel engine vehicles.[24, 35-36] Noteworthy is the Volkswagen scandal, in which it was shown that cars were programmed to release less NO_x under testing conditions than in realistic conditions on the road.[37]

3.1.2 The problem with NOₓ

Irrespective of source, more than 90% of NO_x emissions is NO.[38] NO is a toxic gas which is considered a harmful air pollutant and which may react with oxygen to create NO_2.[39-40] Although both NO and NO_2 are toxic, NO_2 is the far more harmful pollutant.[39]

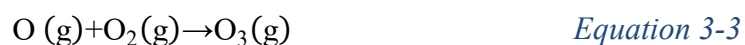NO_2 causes several negative health effects, though affects people in risk groups, such as the elderly, children, or people with respiratory diseases more adversely, even at low concentrations.[36] NO_2 may exacerbate pollen allergy and lung function for people with asthma at concentrations greater than 400 $\mu g/m^3$ when exposed over an hour.[36] Additionally, when exposed for an hour to concentrations above 1880 $\mu g/m^3$, people without pre-existing conditions may experience coughing and irritation of the airways and lungs.[36]

Additionally, NO_2 is one factor contributing to acid rain in the reaction between NO_2 and H_2O in O_2, shown in Equation 3-1.[21] Acid rain causes acidification of lakes and soil, in addition to deterioration of marble and sandstone.[40] This may in turn cause deforestation and the death of fish and other organisms.[21]

$$4NO_2(g)+2H_2O(l)+O_2(g) \rightarrow 4HNO_3(aq) \qquad \textit{Equation 3-1}$$

NO_2 may also react with oxygen in a set of elementary reactions, shown in Equation 3-2, Equation 3-3 and Equation 3-4.[40]

$$NO_2(g) \overset{hv}{\rightarrow} NO\ (g)+O(g) \qquad \textit{Equation 3-2}$$

$$O\ (g)+O_2(g) \rightarrow O_3(g) \qquad \textit{Equation 3-3}$$

$$2NO(g)+O_2(g) \rightarrow 2NO_2(g) \qquad \textit{Equation 3-4}$$

Summing the above three reactions, the net reaction yields ozone as shown in Equation 3-5.[40]

$$3O_2(g) \rightarrow 2O_3(g) \qquad \textit{Equation 3-5}$$

This ozone may then react with NO to give NO_2 and O_2, or react with excess hydrocarbons. Similarly, NO_2 may react with hydrocarbons to yield photochemical smog.[40-41]

Ground level ozone is an irritant which is a part of photochemical smog, and is toxic at high levels.[34] At 0.15 ppm, it causes coughing and irritation of the respiratory system, among other things.[34] It also causes damage to materials like rubber, and is toxic to plants.[34]

Because of the harmful effects of NO_x, there are clear reasons to want to reduce NO_x air pollution. Zeolites and zeotypes are often used as support materials for NO_x reduction catalysts.

3.2 The structure and properties of zeolites and zeotypes

Zeolites and zeotypes belong to a class of materials with beneficial properties for catalysis. These materials are considered as catalysts for converting NO_x into N_2.[30, 42]

Zeolites are made of connected $[SiO_4]^{4-}$ and $[AlO_4]^{5-}$ tetrahedra, where the tetrahedrally coordinated metal is called T-atom. An example of a $[SiO_4]^{4-}$ tetrahedron is given in Figure 3-2.
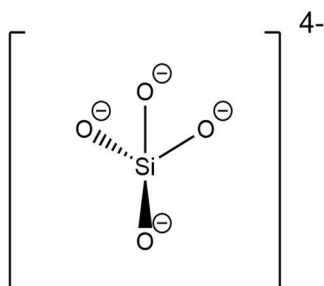
Figure 3-2: $[SiO_4]^{4-}$ tetrahedron

These connected tetrahedra may yield highly crystalline microporous frameworks with repeating porous structure.[43] When Al substitutes Si in the framework structure, the total negative charge of the zeolite grows by one.[43] This charge is balanced by counterions like Na^+, K^+, Ca^+ and Mg^{2+}.[44] These counterions may be replaced by other ions like Ag^+ and Cu^{2+} during ion exchange, while still maintaining electroneutrality. It may also be balanced by protons, which increases the so-called Brønsted-acidity of the zeolite by introducing acid sites.[43] This is called the H-form of zeolites. Brønsted-acidity may increase or decrease the ability of a zeolite to interact with other materials.[43] A Brønsted acid site is illustrated in Figure 3-3.

Figure 3-3: A 2D representation of part of a zeolite structure in H-form.

On the other hand, zeotypes exhibit many of the same characteristics as zeolites; however, have different T-atoms such as P. This is demonstrated in Figure 3-4. For instance, phosphorous in the form of $[PO_4]^{3-}$ tetrahedra may replace silicon in the zeotype structure, which will increase the overall charge of the zeotype by one.[43] This may balance a negative charge brought about by aluminium.
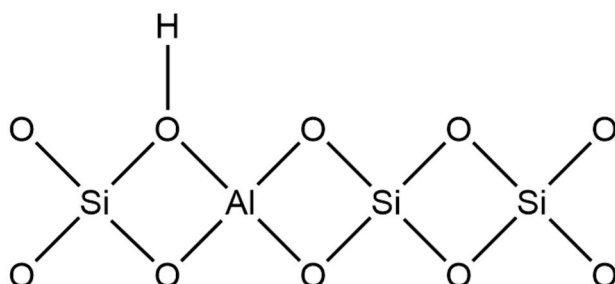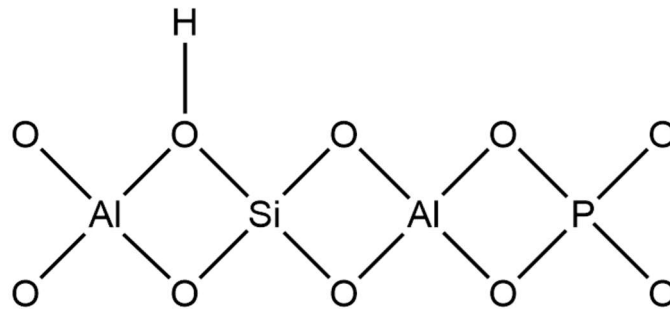

Figure 3-4: A 2D representation of part of a zeotype structure in H-form.

On a larger scale, zeolites and zeotypes are highly crystalline microporous materials.[43] The pore systems may have different dimensionalities. In a one-dimensional system, the pore channels are only available along one axis, i.e. the x-axis.[43] Analogously, for two- and three-dimensional systems, the pore channels are available along two- and three axes respectively.[45]

The type of porosity in zeolites and zeotypes also vary. Micropores are defined as pores smaller than 20 Å in diameter.[43, 46] If the pore size ranges between 20 and 500 Å, the material is mesoporous.[43, 46] Due to their high surface areas, zeolites and zeotypes are ideal for use in catalysis as it allows high dispersion of transition metals, which in turn can catalyse reactions.[43] The same porosity affects which products may form in the pores.[47-48] This is called shape selectivity, and is illustrated in Figure 3-5. Shape selectivity may affect the products in several ways:[47-48]

(a) The reactant size and diffusion rate determine whether the reactant may diffuse into the pores.

(b) The size of the transition state must be accommodated by the pores. If the transition state is too large relative to the pores, the transition state will be destabilized and not likely form.

(c) The product size and diffusion rate determine whether the product may diffuse out of the pores. If the product is too large, it will remain and clog the pores.

By fine tuning the size of pores and cavities in zeolites and zeotypes, more specific reactions may be achieved.[48] However, smaller pores are more prone to coking or clogging of pores, where carbonaceous deposits may remain.[32, 49 43]
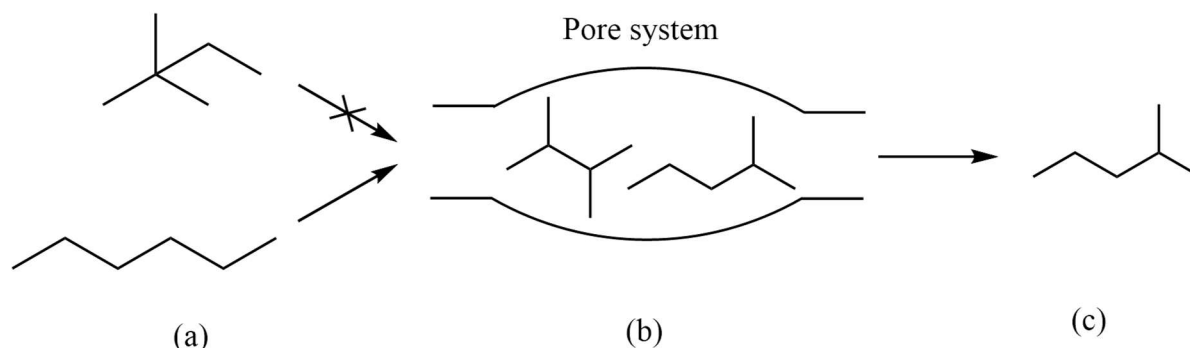

Figure 3-5: Representation of (a) reactant shape selectivity, (b) transition state shape selectivity and (c) product shape selectivity for a hypothetical hydrocarbon isomerization reaction.

For the sake of brevity, the word "zeotypes" will be used to refer to all the frameworks treated in this master thesis. Furthermore, a capital Z is also used as a shorthand of the word "zeotypes". In this sense, Ag:Z refers to zeotypes ion exchanged with silver.

3.2.1 Zeotypes used in this thesis

In this thesis, the zeotypes mordenite, ZSM-5 and SAPO-34 have been investigated. ZSM-5 was provided by Zeolyst international (SiO_2/Al_2O_3=30, CBV 3024E). The supplier of mordenite is not known. SAPO-34 was obtained in two forms; conventional and hierarchical. The conventional SAPO-34 was provided by M. Sc. Joakim Tafjord, whereas the hierarchical SAPO-34 was provided by Ph. D. candidate Guro Sørli; both in the same research group as the author. What follows is a short summary of their properties. These properties are presented in Table 3-1.

Table 3-1: The properties of zeotypes used in this thesis.[1] The largest pore opening refers to the largest diameter of a sphere that can diffuse along the structure. Conv and Hier refers to conventional and hierarchical respectively.

Zeotype	Framework code	Largest pore diameter (/Å)	Pore sizes (/# T atoms)	Relative	Dimensionality
SAPO-34 Conv	CHA	3.72	8, 6, 4	Small	3
ZSM-5	MFI	4.7	10, 6, 5, 4	Medium	3
Mordenite	MOR	6.45	12, 8, 5, 4	Large	2
SAPO-34 Hier	CHA	meso	8, 6, 4, meso	Meso+small	3

The pore sizes of the MOR, MFI and CHA framework structures are illustrated in Figure 3-6 (a)-(c). Among the studied zeotypes, the pore size decreases in order of SAPO-34 Hierarchical>mordenite>ZSM-5>SAPO-34 Conventional.

20 Å
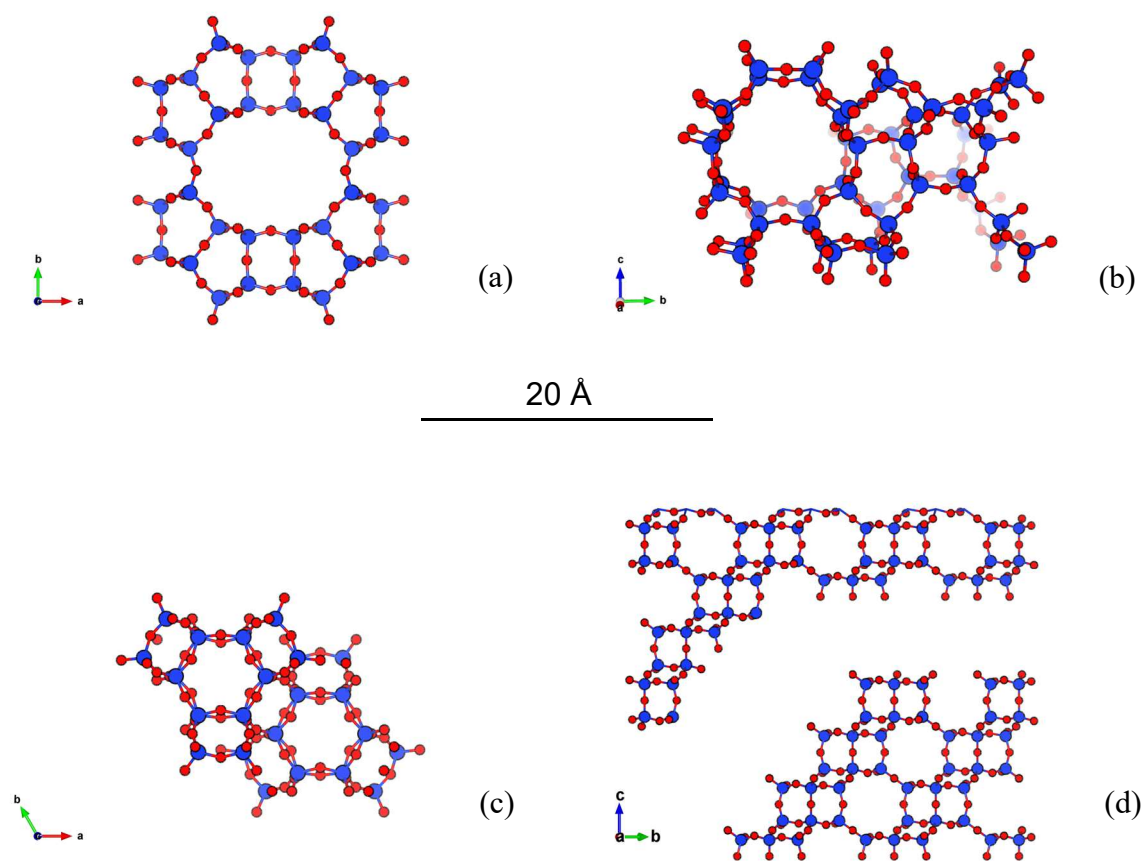
Figure 3-6: Framework images of (a) MOR, projected along [001], (b) MFI, projected along [100] and (c) CHA, projected along [001], and (d) an illustration of SAPO-34 Hier, projected along [100]. Framework images created with Vesta. (d) is not to scale.

Contrary to the other zeotypes, the CHA-framework of SAPO-34 contains so-called cages, in which the inner diameter is 7.37 Å.[1] This is far greater than the pore opening by nearly a factor of 2, and is illustrated in Figure 3-7.[1]
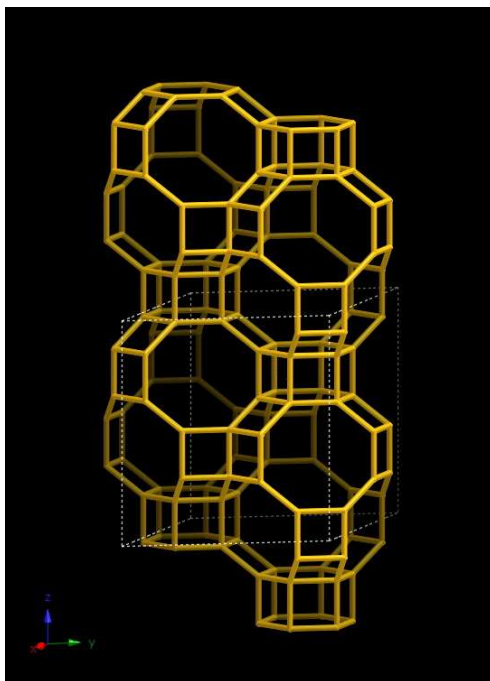
Figure 3-7: CHA framework image, viewed normal to [001].

Figure used with permission by Ch. Baerlocher and L.B. McCusker[1], Database of Zeolite Structures: http://www.iza-structure.org/databases/

The difference between SAPO-34 Conv, which has the conventional structure, and SAPO-34 Hier, which has a hierarchical structure, is the size of pores. SAPO-34 Hier is based on the same framework as conventional SAPO-34, however has porosity at mesoscale, which have been introduced to the microporous framework.[49] This is illustrated in Figure 3-6 (d) and Figure 3-8. In microporous structures, diffusional limitations may render the inner part of micropores unavailable to larger reactants by diffusional limitations.[49] Through introduction of mesopores into microporous structures, often denoted superhighways, hierarchical zeotypes may allow for increased mass transport and simultaneous increased efficiency of the micropores.[49]

The hierarchical SAPO-34 contains mesopores available from the surface of the zeotype in addition to micropores. This is illustrated in Figure 3-8 (c).
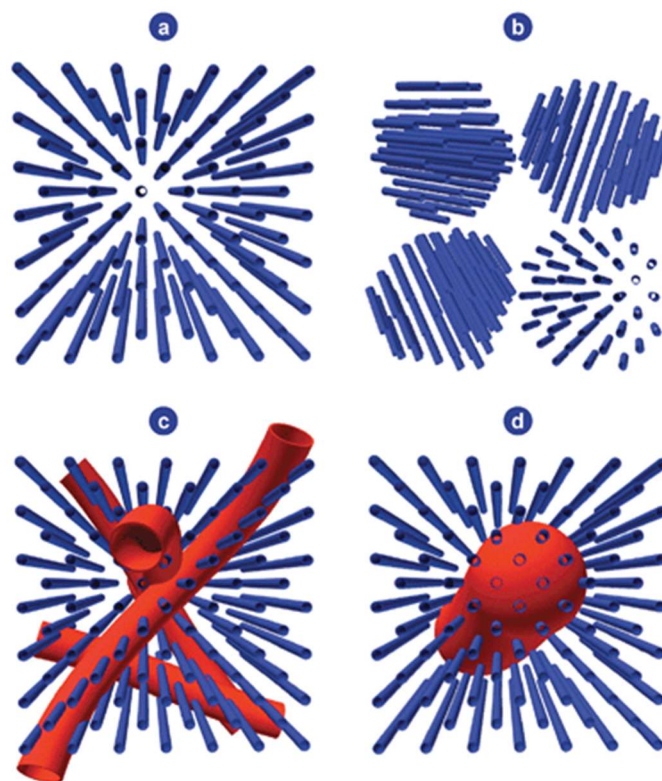
Figure 3-8: Illustration of conventional and hierarchical frameworks. (a) Micropores, as illustrated by the aligned rods. This is a conventional framework (b) nanocrystals with interparticle voids. (c) Mesopores available from the surface and (d) mesovoids in the middle of the microporous network.

Reproduced from [4] with permission of The Royal Society of Chemistry.
http://dx.doi.org/10.1039/B809030K

3.3 Selective catalytic reduction with hydrocarbons (HC-SCR)

The reduction of NO_x to N_2 is thermodynamically favourable below 900°C, however does not happen appreciably under noncatalyzed conditions due to high activation energy.[42] An alternative to direct reduction of NO_x is selective catalytic reduction (SCR), which aims to selectively reduce NO_x to N_2 using a reductant.[29] For SCR catalysts, a high NO_x to N_2 conversion is desired.

In industry and larger vehicles, ammonia or urea is used as a reductant, with good results.[50] For example, a 10% Fe – 10% Mn/TiO_2 catalyst has nearly 100% conversion of NO_x at 120 °C.[51] Employing urea in vehicles is unpractical for several reasons, however, such as necessitating a separate storage tank and increased transport of chemicals. The fact that urea freezes at -11°C further complicates this effort in countries with colder climates.[52]

An alternative is HC-SCR, which aims to utilize leftover hydrocarbons in vehicle exhaust gases to drive the SCR of NO_x.[29] With propene as an example, three simplified reactions take place during HC-SCR as shown below.[3]

In Equation 3-6, NO is oxidized to NO_2. This would take place on the oxidative function of the zeotype supported metal.[3]

$$2NO(g)+O_2(g) \rightarrow 2NO_2(g) \qquad \textit{Equation 3-6}$$

An unwanted reaction may also take place on the oxidative function, namely the direct oxidation of the hydrocarbon as shown in Equation 3-7 with propene.[3] This is undesired, as it leaves less unreacted hydrocarbon for the reduction of NO_2.[10]

$$2C_3H_6(g)+9O_2\ (g) \rightarrow 6CO_2(g)+6H_2O(g) \qquad \textit{Equation 3-7}$$
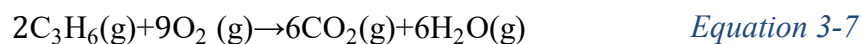
Finally, the selective catalytic reduction of NO_2 into N_2 with propene is shown in Equation 3-8.[3] This would, in turn, occur at the reductive function of the catalyst.

$$4NO_2(g)+2C_3H_6(g)+5O_2(g) \rightarrow 2N_2(g)+6CO_2(g)+6H_2O \qquad \textit{Equation 3-8}$$
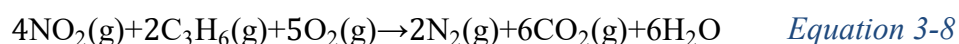
It should be noted that the reactions are, in part, the ideal case. Under realistic conditions, a considerable amount of NO_x may be converted to N_2O, or an incomplete oxidation of propene may yield CO.

3.4 Metal loaded zeotypes for HC-SCR

Metal containing zeotypes have proven useful for HC-SCR due to their activity for this reaction.[29] For instance, supported noble metals such as Pt are active at low temperatures, however Pt is expensive and produces considerable amounts of N_2O.[53] This has been attempted amended by using Ag, which in a mechanical mixture with zeotype supported Pt has seen synergistic effects compared to the separate Ag:Z and Pt:Z.[10] Conversely, many Cu ion exchanged zeotypes show varying degree of activity, but mainly at temperatures at or above 350°C.[7, 31, 54-55] The following section looks closer at suggested detailed reaction mechanisms for HC-SCR, the current state of Ag and Cu in HC-SCR, the effect of mechanical mixing and the effect of simultaneous ion exchange with two metals. It must be noted that reported results for HC-SCR almost certainly employ different reaction conditions, and that results may therefore not be directly comparable.

3.4.1 Reaction mechanism of HC-SCR

Several reaction mechanisms have been proposed for HC-SCR using metal loaded catalysts. A general reaction mechanism, proposed by Gorce, et al. [56] is presented in Figure 3-9. This mechanism was suggested following study on a Ce and Zr oxide with propene.[56]
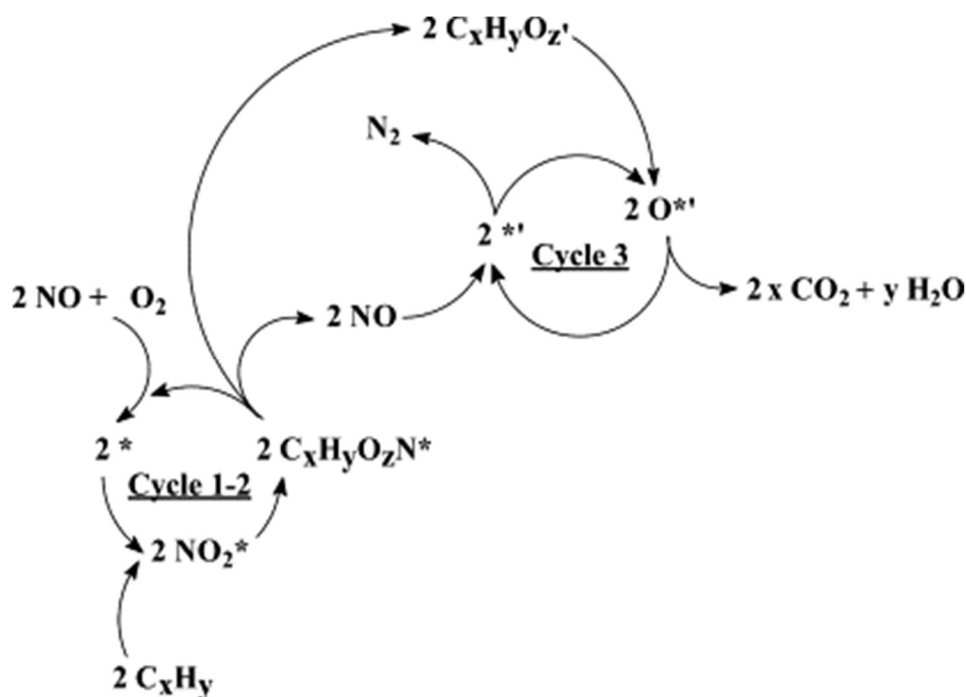
Figure 3-9: Suggested reaction mechanism for HC-SCR.

Reprinted from Applied Catalysis B: Environmental, Vol 54, Olivier Gorce, François Baudin, Cyril Thomas, Patrick Da Costa, Gérald Djéga-Mariadassou, On the role of organic nitrogen-containing species as intermediates in the hydrocarbon-assisted SCR of NOx, Pages 69-84, Copyright 2004, with permission from Elsevier

The reaction mechanism suggests an initial oxidation of NO to NO_2, followed by the formation of an R-NO_x species which is thought to react to yield NO and an oxygenated hydrocarbon.[56] This suggests the presence of NO_2 as an intermediate.[56] It is further corroborated by the increased activity of Ce:ZSM-5 by using NO_2 instead of NO as model gas for NO_x.[3] At higher temperatures, it is noted, the fast interconversion between NO and NO_2 is thought to remove differences between using either gas in the feed.[3] The oxygenated species is then thought to react with adsorbed oxygen left over from NO conversion into N_2, thus completing the cycle.[56]

A paper from 2009 looking closer at HC-SCR with propene on metal ion exchanged ZSM-5 indicates that both NO_2 and oxygenated HC are intermediates, however also suggest the presence of an adsorbed amine species.[57] This is further corroborated by a recent paper by Moreno-González, et al. [55] looking closer at the effect of Cu zeolite catalysts for HC-SCR,

however with propane as reductant. It is suggested that the organonitric compounds reacts with water to form ammonium, which in turn reacts similar to ammonium-SCR.[55]

3.4.2 Cu in HC-SCR

As has already been shown, transition metals are often supported on zeolite to function as catalysts in HC-SCR. In this regard, Cu ion exchanged zeotypes have been widely studied ever since Iwamoto, et al. [30] demonstrated the high activity of Cu:ZSM-5 in HC-SCR. The activity of Cu zeotypes are clearly seen to vary with the zeotype used, however; as seen in a report by Torre-Abreu, et al. [31] which compares the HC-SCR $deNO_x$ activity of the zeotypes Cu:MOR, Cu:Y and Cu:MFI. In this case, the activity of Cu:MFI is seen to be the most active independent of acidity, followed by Cu:MOR and Cu:Y.[31] Similar $deNO_x$ results with Cu:ZSM-5 show $deNO_x$ conversion of 63% at 350°C.[7] A realistic fuel feed, however, contains both water and SO_2.[30, 58] The same Cu catalyst, then, is prone to reduced activity in the presence of water, which reduces its conversion at 350°C to 2%.[7] Research by Iwamoto, et al. [30] suggest that the effect of SO_2 is not equally detrimental, as the NO_x conversion in their experiments was lowered from 100% to 85% at 500°C.

A more recent report, focusing on the effect water has on Cu:Z over time, notes how water at high temperatures aids in converting the metastable zeotypic frameworks to more stable crystalline phases, thereby reducing porosity.[58] This can in part be prevented by using small pore zeotypes for Cu:Z in SCR.[58]

With propene and Cu:ZSM-5, one proposed mechanism includes a full redox cycle in which Cu(II) is first reduced to Cu(I) by adsorbing propene, and subsequently re-oxidized to Cu(II) by oxygen.[57] Conflicting evidence exist for different Cu:Z and hydrocarbons; a similar paper suggests that Cu(I) is oxidized to Cu(II) by adsorption of nitrate, and then turned back into Cu(I) upon the reaction with ammonia in the presence of propane.[55]

3.4.3 Ag in HC-SCR

Several reports showcase the deNO$_x$ activity of supported silver.[3, 50, 53, 59-64] More recent research with Al$_2$O$_3$ supported Ag shows very high HC-SCR performance with ethanol as the reductant.[65] The addition of H$_2$ in HC-SCR with Ag is also studied.[64] Chajar, et al. [7] report NO to N$_2$ conversions without water of 13% and 57% at 350°C and 500°C respectively with Ag:ZSM-5. The conversion of NO into N$_2$ in the presence of water is reported to be 12% and 54% at 350°C and 500°C respectively, a miniscule change as opposed to the detrimental effect water has on Cu:ZSM-5.[7] The hydrothermal stability showcases one of the more attractive properties of using supported silver in HC-SCR, and also in part why it has been considered in this thesis.

In a report by Martens et al, the effect of molecular sieving in zeotypes with octane and isooctane is studied. In the case of Ag:MOR in octane, the maximum of NO$_x$ into N$_2$ conversion of 13% is seen at 360°C, consistent with Ag:ZSM-5 results.[7, 10] Although the maximum conversion value remains the same by using isooctane, the temperature for maximum conversion shifts to 460°C. With Ag:CHA, the activity with octane is shown to reach 35% at 500°C. Both cases demonstrate low NO$_x$ conversion values at low temperatures; this is attributed to the lack of an NO oxidation function.[10]

The reaction mechanism of Ag containing zeotypes has also been studied. It has been proposed by Mathisen, et al. [62] that Ag$^+$ in ion exchanged Ag:ZSM-5 and Ag:SAPO-5 form Ag nanoparticles in the presence of propene during HC-SCR. The resulting Ag nanoparticles are thought to be reoxidized to Ag$^+$ upon treatment with NO.[62] Differences in activities between Ag:ZSM-5 and Ag:SAPO-5 are thought to be caused by the degree to which metallic Ag is formed; as Ag$^+$ is more effectively reduced by propene in Ag:SAPO-5 than Ag:ZSM-5.[62]

3.4.4 Mechanical mixing of zeotypes: The dual pore concept

Zeotypes of varying pore sizes may act as molecular sieves, restricting the access of larger species like bulky hydrocarbons.[10, 31, 58, 66] The dual pore concept, which is illustrated in Figure 3-10, entails separating the oxidative- and reductive functions in a zeotype system with two different pore sizes.[3] By restricting the pore size of the oxidative function, the small molecules NO and O_2 can readily diffuse into the pores and be converted to NO_2 on the oxidative function, simultaneously limiting the direct oxidation of larger hydrocarbons.[3] If this effect is combined with a metal with reductive function embedded in large pores, large hydrocarbons may thereby reduce NO_2 to N_2.[3] This effect has been studied by considering the difference between a straight chain hydrocarbon and bulkier hydrocarbons with the same amount of carbon atoms.[10]
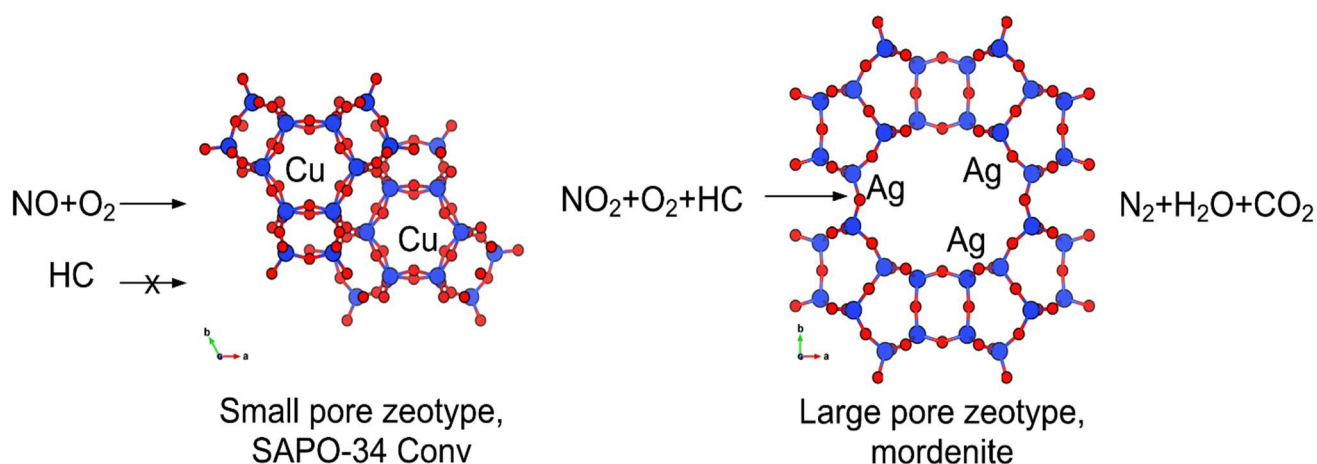
Figure 3-10: Illustration of the dual pore concept. Not to scale. Adapted from [3]. The dual pore concept is illustrated with a Cu containing SAPO-34 Conv, which has small pores, and an Ag containing mordenite, which has large pores. Shape selectivity is thought to restrict the entry of the hydrocarbon into the SAPO-34 Conv, whereas NO and O_2 can freely enter and be converted to NO_2. In the mordenite, all species may enter and react to form nitrogen gas, water and carbon dioxide. CHA and MOR framework structures created with VESTA.

One paper studying the difference between using octane and isooctane in a dual pore system, found a synergistic effect of the bulkier hydrocarbon.[10] Here, Pt in small pores effectively oxidizes NO into NO_2, whereas the pore size hinders the direct oxidation of the hydrocarbon.[10] Furthermore, the large pore Ag:Z facilitated the reduction of NO_2 into N_2.[10] Here, as in other sources, pore size limited hydrocarbon entry into the small pore zeotype, depending on HC size.[10, 67] This effect was however most pronounced in the temperature range of 200-400°C[10] Furthermore, they found that for a mechanically mixed catalyst made of 0.5Pt/H-FER and 5Ag:MOR, NO_2 only appeared as a reaction product after the conversion maximum at 260°C.[10]

The sample shows considerable direct HC oxidation activity above these temperatures, which is used to explain the decrease in NO_x conversion.

A similar paper considers the mechanical mixture of CoFER and H-ZSM-5. Similar to the work already mentioned with mechanically mixed zeotypes, an activity window is seen between 300°C and 400°C.[9] In this case, however, the activity may be attributed to the activity of H-ZSM-5, whose NO_x conversion is higher and shows a similar trend to that of the mixed catalyst.[9] Nevertheless, the dual pore concept is thought to yield synergistic effects for $deNO_x$ conversion owed to the separation of the oxidative and reductive functions.

3.4.5 Simultaneous metal ion exchange: The two-cation effect

The two-cation effect is the effect of two different cations in the same zeotype. This master's thesis is in part concerned with the simultaneous ion exchange of Ag and Cu into zeotypes. Wang, et al. [68] report on the simultaneous ion exchange on CuFe:Zeolite Beta and SSZ-15, and compares the catalysts to their singly ion exchanged counterparts in ammonium-SCR with propene. Their results show no notable synergistic effect of the simultaneous ion exchange for ammonium-SCR.[68]

Based on earlier work, the simultaneous ion exchange of Ag and Cu into Zeolite Y required a 4:1 relationship of Ag:Cu by mass in the solutions to yield 0.7 wt% of Ag and Cu each; a 1:1 relationship of Ag:Cu in the zeolite.[69] As a result, Cu occupies different positions in simultaneously ion exchanged Zeolite Y compared to Cu:Zeolite Y.[69] In this case, the simultaneously ion exchanged AgCu:Zeolite Y performed poorly during HC-SCR with propene, having a maximum activity of 4% in the temperature range 250-500°C.

To the best of the author's knowledge, the simultaneous ion exchange of two metals has not been studied further.

With respect to the above discussion, the $deNO_x$ conversion and activity of mechanically mixed zeotypes with small, medium, large and mesopores will be investigated. These will be compared to simultaneously and separately ion exchanged zeotypes with Ag and Cu to determine potential synergistic effects of the dual pore concept and simultaneous exchange.

3.5 Powder X-ray diffraction (XRD)

Zeotypes may collapse during ion exchange, which reduces the crystallinity.[43] This has been seen for Cu:SAPO-34 in particular, where it is caused by irreversible hydrolysis.[70] As a result, all samples have been studied by XRD before and after ion exchange.

X-ray diffraction is a technique used for analysing and verifying crystallinity in homogeneous samples.[71] In powder X-ray diffraction, the sample is polycrystalline, containing a multitude of small crystallites oriented randomly.[71] When the sample is irradiated with X-rays, the diffracted rays merge together to create a cone of diffraction which is measured by the detector.[71] As such, peaks will be observed when positive interference occurs.[71] For materials with the same crystal structure, an equal XRD pattern is observed in the ideal case.[71]

3.6 Inductively coupled plasma – Mass spectrometry (ICP-MS)

The samples in this study were ion exchanged with goal of achieving 5 wt% of each metal (Ag, Cu). However, the metal content may differ despite using equal concentrations for ion exchange. To determine the resulting metal contents after ion exchange, ICP-MS has been employed.

ICP-MS is a technique that can be used to simultaneously determine over 70 elements with very high precision.[72] This method of atomic mass spectrometry uses high temperature argon plasma to ionize samples, before the contents are differentiated based on their mass-to-charge (m/z) ratio using a quadrupole before promptly being detected in the mass spectrometer.

4.0   Experimental

In the section to follow, the sample preparation method, instrumental setup and method for catalytic testing will be explored. Three categories of samples, the significance of which has been seen in section 3.4, have been prepared for HC-SCR by ion exchange. These include

- Separately ion exchanged zeotypes with either Ag or Cu, denoted Me:Z
- Mechanically mixed Ag and Cu ion exchanged zeotypes, shown as [Ag+Cu]:Z or Ag:Z+Cu:Z. The former indicates that Ag and Cu are in the same zeotype, whereas the latter indicates that Ag and Cu are present in different zeotypes.
- Simultaneously ion exchanged Ag and Cu zeotypes, or AgCu:Z

The purpose of the separately and simultaneously ion exchanged samples is to contrast the mechanically mixed samples and their $deNO_x$ conversions. As such, the degree of activity which is attributable to the dual pore concept and porosity may be separated from the activities of Ag:Z, Cu:Z and AgCu:Z.

The prepared samples are shown in Table 4-1, along with the pore position of each metal and whether the catalyst is a mechanical mixture. Ag:Z and Cu:Z have also been prepared as references for each zeotype studied, but are not included in this table.

Table 4-1: Overview of ion exchanged and catalytically tested samples with respect to framework, metal, size of pore where each metal is situated and whether the sample is a mechanical mixture.

Catalyst	Element position		
	Ag	Cu	Mix
Ag:ZSM-5 + Cu:SAPO-34 Conv	Medium	Small	Yes
Ag:ZSM-5 + Cu:MOR	Medium	Large	Yes
Ag:MOR + Cu:ZSM-5	Large	Medium	Yes
[Ag+Cu]:SAPO-34 Conv	Small	Small	Yes
AgCu:SAPO-34 Conv	Small	Small	No
[Ag+Cu]:ZSM-5	Medium	Medium	Yes
AgCu:ZSM-5	Medium	Medium	No
[Ag+Cu]:MOR	Large	Large	Yes
AgCu:MOR	Large	Large	No
[Ag+Cu]:SAPO-34 Hier	Meso+small	Meso+small	Yes
AgCu:SAPO-34 Hier	Meso+small	Meso+small	No

4.1 Ion Exchange of samples

During ion exchange, the zeotype is added to a beaker along with 30 mL copper tetraamine solution or $AgNO_3$ solution per gram of zeotype. The mixture is stirred in room temperature for 24 hours. Following this, the sample is centrifuged two times and washed with H_2O two times. The samples are thereby dried at temperatures ranging from 40°C to 110°C for 24 hours.

The solutions used in the ion exchange aimed at achieving 5 wt% metal content in the zeotypes. To achieve this, two different $AgNO_3$ concentrations were tried out, namely 0.053 and 0.071 mol/L. The different concentrations did not yield substantially different Ag content in the resulting samples. Copper tetraamine solution (0.030 mol/L) was used for the Cu:Z. NH_3 (5 mol/L) was added to $Cu(NO_3)_2*3H_2O$ (0.030 mol/L) to prepare the copper tetraamine solution as shown in Figure 4-1.

Figure 4-1: Copper tetraamine solution (0.030 mol/L)

During the simultaneous ion exchange for AgCu:Z, a weight ratio of 4:1 of Ag:Cu in solution was used, mirroring the work of Delic.[69] In their work on zeolite Y, this ratio of ions yielded a relative wt% of Ag:Cu of 1:1.[69]

For the simultaneous ion exchange with Cu and Ag, a solution of both copper tetraamine (0.030 mol/L) and $AgNO_3$ (0.071 mol/L) was used. NH_3 (5 mol/L) was added to the precursor solution, analogous to the addition to the $Cu(NO_3)_2*3H_2O$ solution.

4.2 Powder X-ray diffraction instrumentation

XRD was performed on the zeotypes before and after ion exchange in order to verify the crystallinity of the zeotypes after ion exchange due to the potential of structural collapse.[70]

For XRD, a Bruker D8 A25 DaVinci X-ray Diffractometer with CuKα radiation and LynxEye™ SuperSpeed Detector was used. The divergence slit opened automatically, keeping a constant illuminated length of 6 mm on the sample. With these settings, 2θ values between 5 degrees and 60 degrees were scanned with a program with a total duration of 15 minutes. XRD diffractograms have been recorded using identical sample holders, unless otherwise noted.

4.3 ICP-MS instrumentation

Elemental analysis was carried out by Syverin Lierhagen (IKJ), and was performed using an Agilent 8800 ICP Triple Quad to verify the metal contents of ion exchanged zeotypes.

During ICP-MS sample preparation, each sample (10-45 mg) was weighed out in a Teflon tube (25 mL) which had been rinsed three times with deionized water. HNO_3 (concentrated, 1.5 mL) was added, followed by HF (40 wt%, 0.5 g), before the samples were let dissolve. After dissolution, the solution was transferred to a larger Teflon vessel before being diluted with deionized water to a total mass of 216.6 g. A Teflon tube (16 mL) was thereby rinsed three times with the sample solution before being filled with the sample solution. Three blank samples were run to eliminate background noise.

4.4 Catalysis

4.4.1 Instrumentation

A CLD 62 Eco-Physics Chemiluminescence NO/NO_x Analyzer was used to detect changes in NO_x concentration. This was connected to a Nabertherm R50/250/12 tube furnace with a C450 controller. Gases used were NO (1 vol% in He), O_2 (10 vol% in He), propene (2 vol% in He) and argon, all provided by AGA. Propene was used as it is a component of fuel exhaust, and as its use in HC-SCR has been studied in the research group in which the author is part.[73] The instrumentation is illustrated in Figure 4-2.

Upon attempting calibration with NO in helium, the measured NO_x concentration varied wildly. As such, the NO_x analyser was calibrated using NO with balance Ar. Using a total flow of 80 mL/min, the instrument was calibrated at 300 and 400 ppm NO, in addition to each 100 ppm NO-interval between and including 1100 and 2000 ppm.
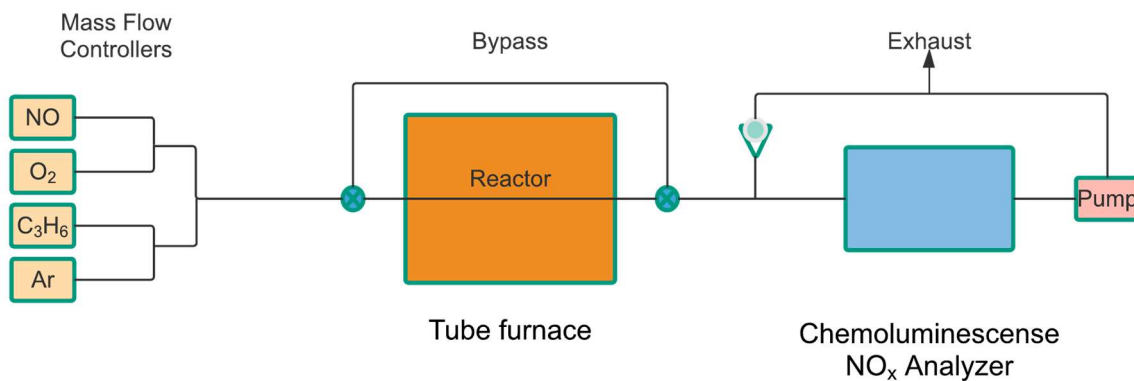

Figure 4-2: Schematic figure showing the instrumentation used for catalytic measurements.

4.4.2   Sample preparation

The sample preparation is illustrated in Figure 4-3. During catalysis, the Ag:Z, Cu:Z and AgCu:Z sample were prepared by pressing each sample to a pellet, before sieving it to yield particle of size between 212 and 425 μm. Of this, 0.150 g is used for catalysis. For the mechanically mixed samples, [Ag+Cu]:Z, 0.225 g of each sample is first weighed out and added to a mortar. As such, in mixed samples, an equal amount of each sample is used. The two samples are mixed in a mortar and thoroughly ground with a pestle. The sample is thereafter treated identically to the unmixed sample, as it is pressed and sieved. 0.150 g of the mechanical mixture is used in catalysis.

0.150 g sample is used to yield a weight hourly space velocity (WHSV) of 171 h^{-1}. This value was chosen to be comparable to a WHSV of 200 h^{-1}, which is used in research performed in the same research group as the author.

After sample preparation, the sample is fixed in a metal tube reactor with quartz wool on either side.
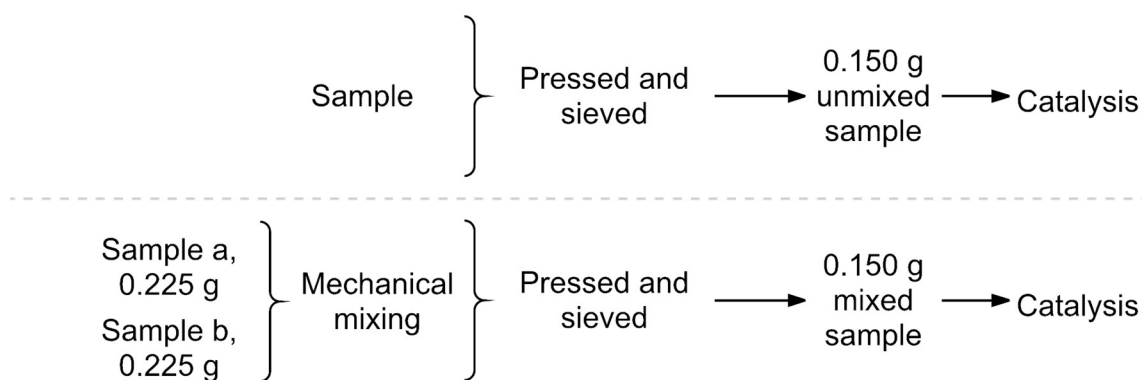
Figure 4-3: A figure contrasting the sample preparation methods for plain samples and mechanically mixed samples.

4.4.3 Catalytic testing

Before catalytic measurements were started, each sample was heated to 500°C with a gas flow of Ar or Ar and O_2. Upon reaching 500°C, the sample was activated in 2 vol% O_2 and 98 vol% Ar as dilution gas, with a total flow of 80 mL/min for 60 minutes. A concentration of 2000 ppm NO, 1200 ppm propene, 2 vol% O_2 and balance Ar as dilution gas, with a total flow of 140 mL/min was used during the catalytic measurements. This gas mixture was chosen to correspond with work done with the same research group.

NO_x conversion was measured for 20 minutes at each 25°C interval between 500°C and 275°C inclusive. The last measured NO_x value at each 25°C interval was chosen as the representative conversion for each temperature, after which the measured concentration of NO_x from the reactor had stabilized. The temperature program and gas concentrations are illustrated in Figure 4-4.
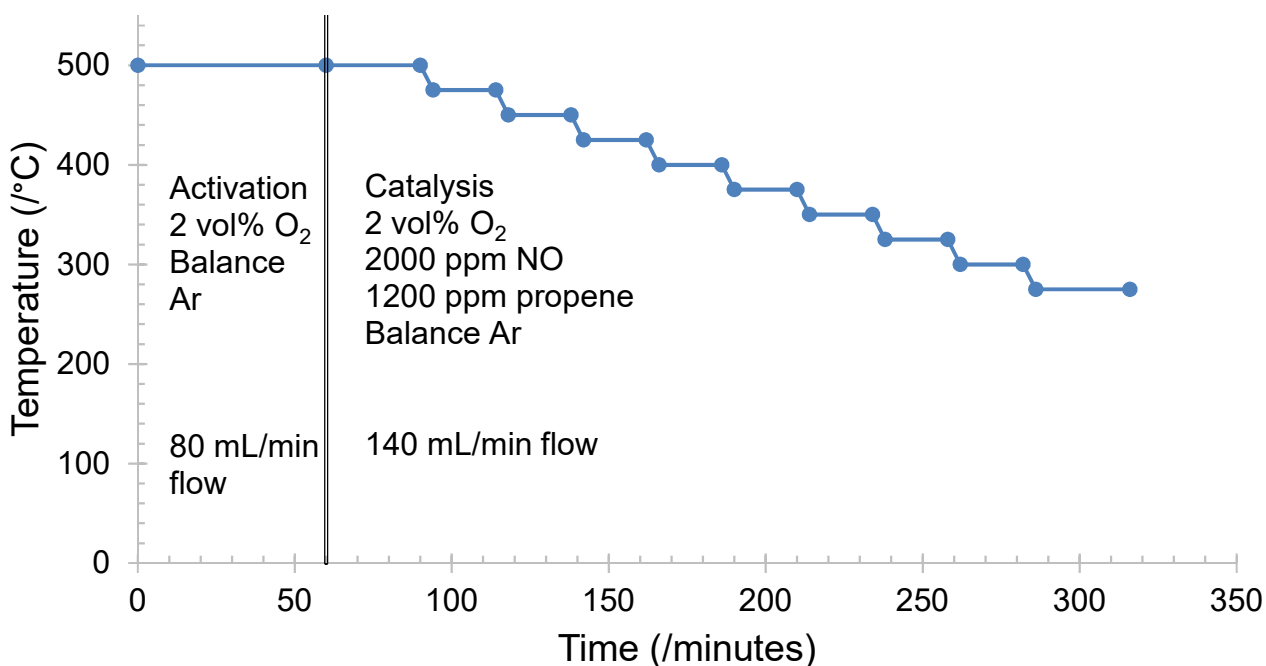

Figure 4-4: Figure showing the temperature program used for the tube furnace during catalytic measurements, and the gas concentrations used. The line at 60 minutes indicates the end of activation and start of bypass measurement and catalysis.

Bypass concentration was measured for 10 minutes at 500°C and 275°C; at the beginning and end of the catalytic testing respectively. For each catalysis, the two bypass concentrations were not equal. As a result, a weighted average was used. The formula for calculating the weighted average is shown in Equation 4-1.

$$NO_{x\text{weighted bypass}}=\left(\frac{500\text{-}T}{225}\right)*BypassEnd+\left(\frac{T\text{-}275}{225}\right)*BypassStart) \qquad \textit{Equation 4-1}$$

Here, T is the temperature, BypassEnd is the bypass NO_x concentration measured at 275°C and BypassStart is the measured bypass NO_x concentration at 500°C. This meant that at temperatures close to the first measured bypass concentration, this bypass value is weighted more heavily.

With respect to the above considerations NO_x conversion was calculated as shown in Equation 4-2.

$$NO_x \text{ conversion}=\frac{NO_{x\text{weighted bypass}}\text{-}NO_{x\text{reactor}}}{NO_{x\text{weighted bypass}}} \qquad \textit{Equation 4-2}$$

After each run, the NO_x concentration data (concentration of NO_x over time) and furnace temperature data (temperature over time) were related to give the concentration of NO_x at the temperature range studied. The activity of the catalysts was thereby plotted. In this master thesis, a sample is deemed active at the temperatures for which the conversion is greater than or equal to 30% NO_x conversion. This is used in activity diagrams, where a capital M indicates the temperature of maximum conversion for each zeotype. Coloured squares indicate for which temperatures and zeotypes the conversion is greater than or equal to 30%.

It is noted how the method used only measures the removal of NO and NO_2, and not their respective conversions into N_2. This was not possible with the instruments used.

5.0   Results

In this section, selected data from characterization by XRD and ICP-MS will first be presented. Then, the NO$_x$ conversion diagrams with focus on the effect of mechanical mixing and the effect of porosity are shown with activity diagrams.

5.1 Characterization

5.1.1   XRD results of calcined and ion exchanged samples

The XRD results for ZSM-5 and mordenite samples show little reduction of crystallinity between the calcined and ion exchanged samples, and are therefore found in Appendix A: Additional XRD results. Diffractograms for SAPO-34 Hier are also found in Appendix A. The XRD-results of SAPO-34 Conv are shown in Figure 5-1. For all SAPO-34 samples, a considerable reduction in crystallinity is seen. Among the conventional samples, the Cu sample has the lowest crystallinity, followed by the AgCu and Ag sample respectively. An analogous effect is seen for the hierarchical samples, albeit the reduction of crystallinity is even greater, and most pronounced for the Ag and AgCu sample. The reduction in crystallinity is in line with what has been found by Gao, et al. [70] regarding irreversible hydrolysis causing the structural collapse of Cu:SAPO-34 Conv samples.
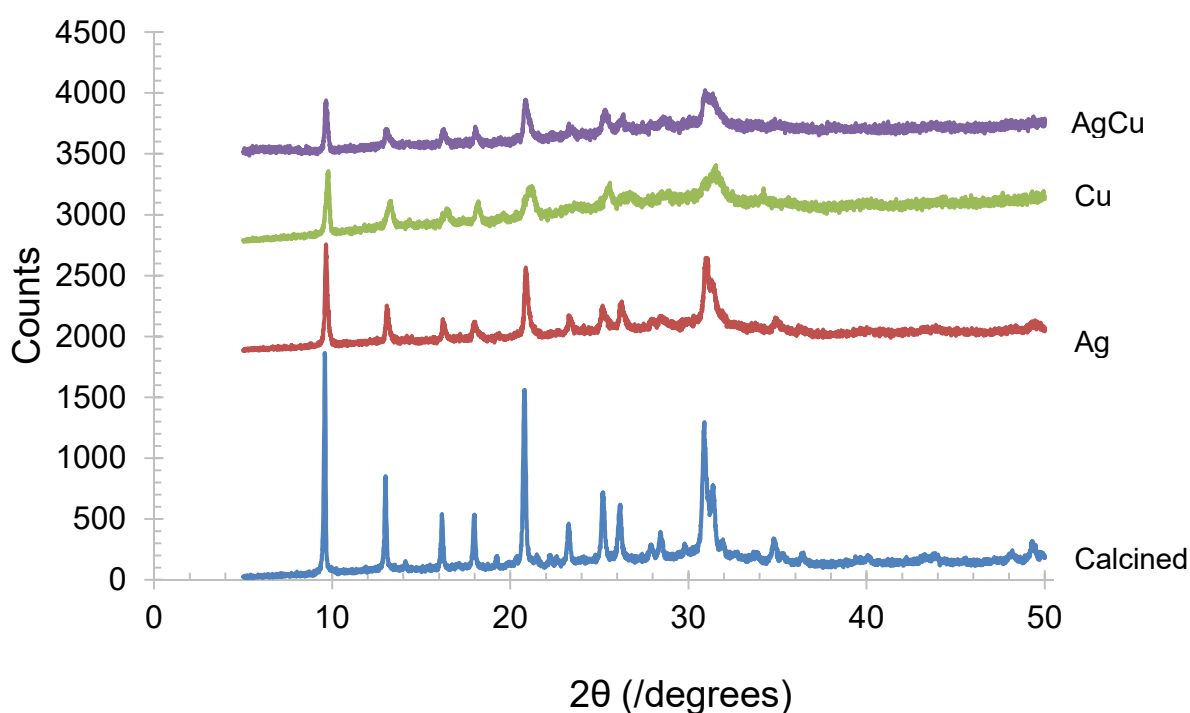
Figure 5-1: Powder XRD-data of selected SAPO-34 Conv samples.

5.1.2   ICP-MS results of ion exchanged samples

Selected results of ICP-MS elemental analysis are shown in Figure 5-2. Several things can be noted. Firstly, the MOR samples contain considerably more Ag than any other zeotype. Secondly, a greater variance is seen in Ag content than for Cu content. Whereas the Cu content varies between 2 wt% and 6 wt%, the Ag content ranged from 2 wt% to 12 wt%. Additionally, AgCu samples have higher total uptake of metal than if one were to sum the Ag and Cu content of Ag:Z and Cu:Z samples respectively. Finally, the Cu content of AgCu:Z is lower than the respective Cu:Z in all cases but SAPO-34 Conv. All ICP-MS results are given in Appendix B: Additional ICP-MS results.
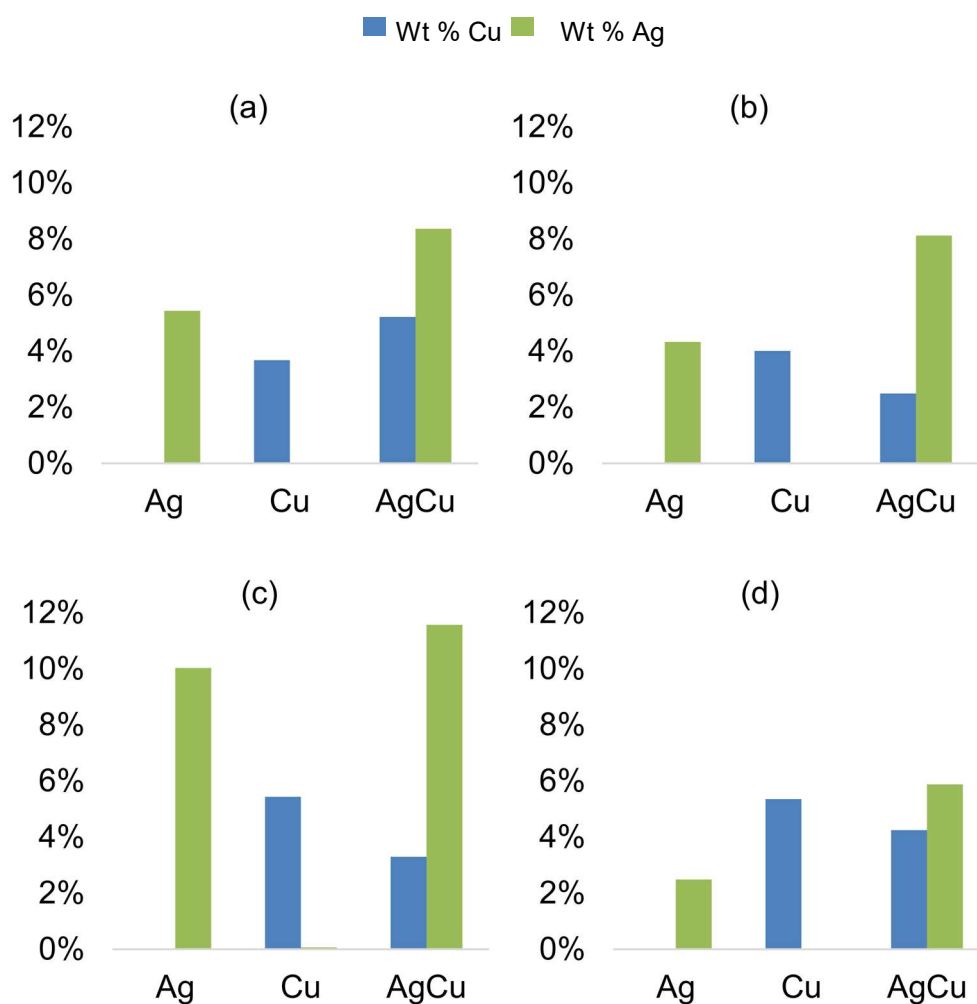
Figure 5-2: ICP-MS results with sample metal contents for (a) SAPO-34 Conv, (b) ZSM-5, (c) MOR and (d) SAPO-34 Hier.

5.2 Catalysis - Effect of mechanical mixing

In this section, the deNO$_x$ results for mechanically mixed zeotypes are presented and compared to reference zeotypes with Ag and Cu. To recap, mechanically mixed zeotypes were prepared by mixing equal parts of Ag:Z and Cu:Z, though the zeotypes may be different. For the first three samples, Ag and Cu are in zeotypes with different pore sizes. This is shown as Ag:Z+Cu:Z. Following this, a comparison of mechanically mixed catalysts with Ag and Cu in same pores are also presented, shown as [Ag+Cu]:Z. This way, the potential benefit of having Cu in small pores and Ag in large pores, as suggested in the dual pore concept, may be determined. The Ag:Z and Cu:Z samples tested and used for mechanically mixed catalysts are considered reference samples in this regard. DeNO$_x$ results of the Ag:Z and Cu:Z reference samples comparing the conversion with different zeotypes are found in Appendix C: Additional deNOx results.

5.2.1   DeNOₓ results for Ag:ZSM-5+Cu:MOR

The first mechanically mixed catalyst, which is made from the medium pore Ag:ZSM-5 and large pore Cu:MOR, performs poorly, with an activity below both of its reference samples and a maximum activity of 6%. These results may be seen in Figure 5-3. This is surprising, considering the high activity of the Cu:MOR reference, which makes up half of the mechanically mixed sample. With these zeotypes, mechanical mixing therefore has a notable negative effect.
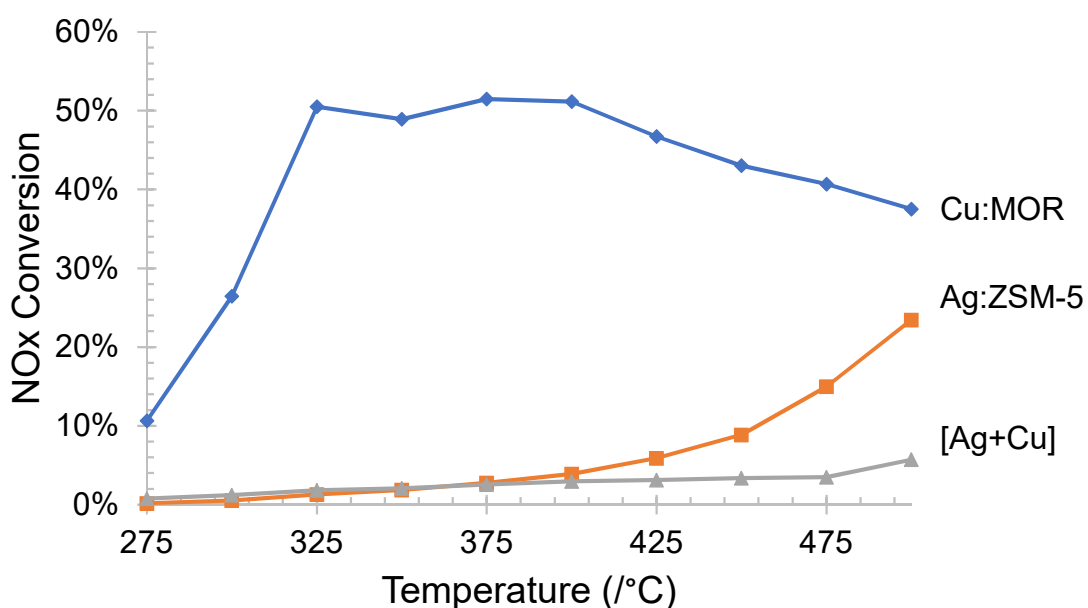
Figure 5-3: DeNOₓ results for Ag:ZSM-5+Cu:MOR and its components. [Ag+Cu] is the mechanical mixture of Ag:ZSM-5 and Cu:MOR.

The activity diagram for these samples is shown in Table 5-1, where it can be seen that the mechanically mixed catalyst has no activity, in stark comparison to the reference sample Cu:MOR, which is active between 325°C and 500°C inclusive.

Table 5-1: Activity diagram for Ag:ZSM-5+Cu:MOR. [Ag+Cu] is the mechanical mixture of Ag:ZSM-5 and Cu:MOR. M indicates temperature for maximum conversion for each zeotype. Colour means that the zeotype is deemed active at that temperature.

Temperature (/°C)	275	300	325	350	375	400	425	450	475	500
Ag:ZSM-5										M
Cu:MOR					M					
[Ag+Cu]										M

5.2.2 DeNOₓ results for Ag:MOR+Cu:ZSM-5

The mixed Ag:MOR+Cu:ZSM-5 is the opposite case to Figure 5-4 as the positions of Ag and Cu are interchanged. Notable differences are seen; for instance, Ag:MOR+Cu:ZSM-5 perform near equal to the high performing Cu:ZSM-5 reference sample at temperatures exceeding 425°C. Although the mechanically mixed sample has the lowest conversion at temperatures below 425°C, these results suggest a notable effect of porosity.
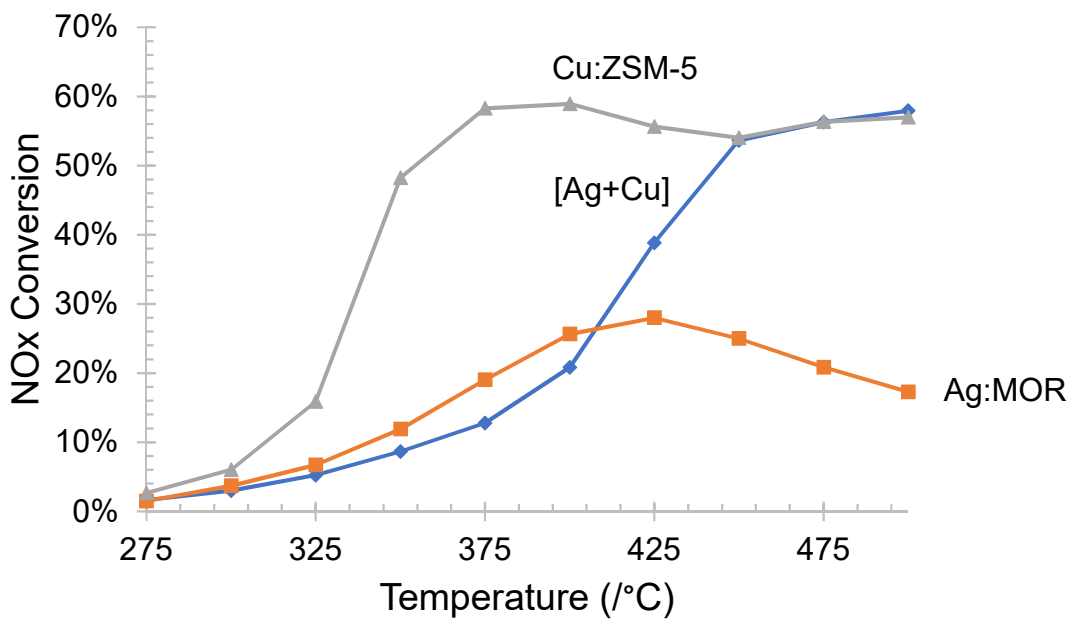
Figure 5-4: DeNOₓ results for Ag:MOR+Cu:ZSM-5 and its components. [Ag+Cu] is the mechanical mixture of Ag:MOR+Cu:ZSM-5.

With respect to Table 5-2, the mechanically mixed sample is seen to have nearly half the activity window that the Cu:ZSM-5 reference has. This is a far larger activity window than were the positions of Ag and Cu in the zeotypes interchanged, though still not an improvement with respect to the Cu:MOR reference seen in Table 5-1.

Table 5-2: Activity diagram for Ag:MOR+Cu:ZSM-5. [Ag+Cu] is the mechanical mixture of Ag:MOR+Cu:ZSM-5.

Temperature (/°C)	275	300	325	350	375	400	425	450	475	500
Ag:MOR							M			
Cu:ZSM-5					M					
[Ag+Cu]										M

5.2.3 DeNOₓ results for Ag:ZSM-5+Cu:SAPO-34 Conv

Figure 5-5 showcases the results with Ag in the medium pore ZSM-5, mechanically mixed with Cu in the small pore SAPO-34 Conv. As seen previously with other mechanical mixed samples, despite the high activity of the Cu:Z reference sample, this mechanical mixture performs poorly. Notably, the mechanically mixed catalyst performs equally to Ag:ZSM-5 at all temperatures except 500°C.
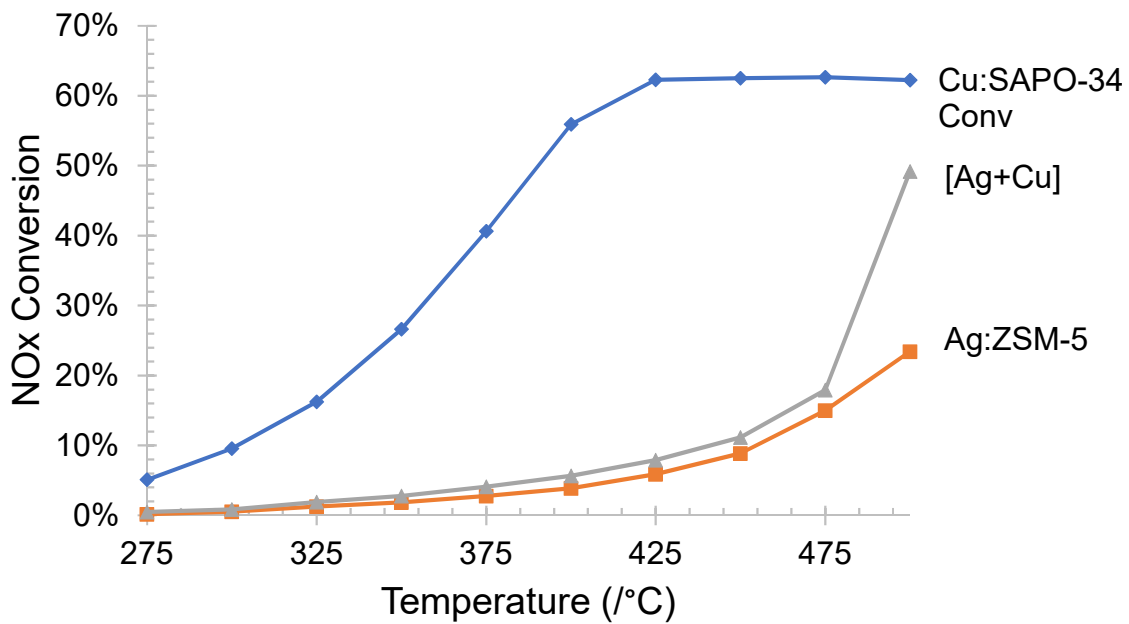
Figure 5-5: DeNOₓ results for Ag:ZSM-5+Cu:SAPO-34 Conv and its components. [Ag+Cu] is the mechanical mixture of Ag:ZSM-5+Cu:SAPO-34 Conv

The low activity of the mechanically mixed catalyst is also reflected in the activity diagram in Table 5-3, as Ag:ZSM-5+Cu:SAPO-34 is only active at 500°C. This is in line with the samples presented thus far in that the mechanically mixed catalyst exhibits low or intermediate activity between that of its Ag:Z and Cu:Z reference.

Table 5-3: Activity diagram for Ag:ZSM-5+Cu:SAPO-34 Conv. [Ag+Cu] is the mechanical mixture of Ag:ZSM-5 + Cu:SAPO-34 Conv

Temperature (/°C)	275	300	325	350	375	400	425	450	475	500
Ag:ZSM-5										M
Cu:SAPO-34 Conv										M
[Ag+Cu]										M

5.2.4 DeNOₓ results for [Ag+Cu]:Zeotypes

The results for mechanically mixed zeotypes, in which Ag:Z and Cu:Z are in the same zeotype, is shown in Figure 5-6. The activity exhibited by [Ag+Cu]:ZSM-5 is 59% at 500°C, and surpasses all the mixed catalysts so far. Notable activity is also seen for MOR, which has its peak activity of 44% at 325°C.
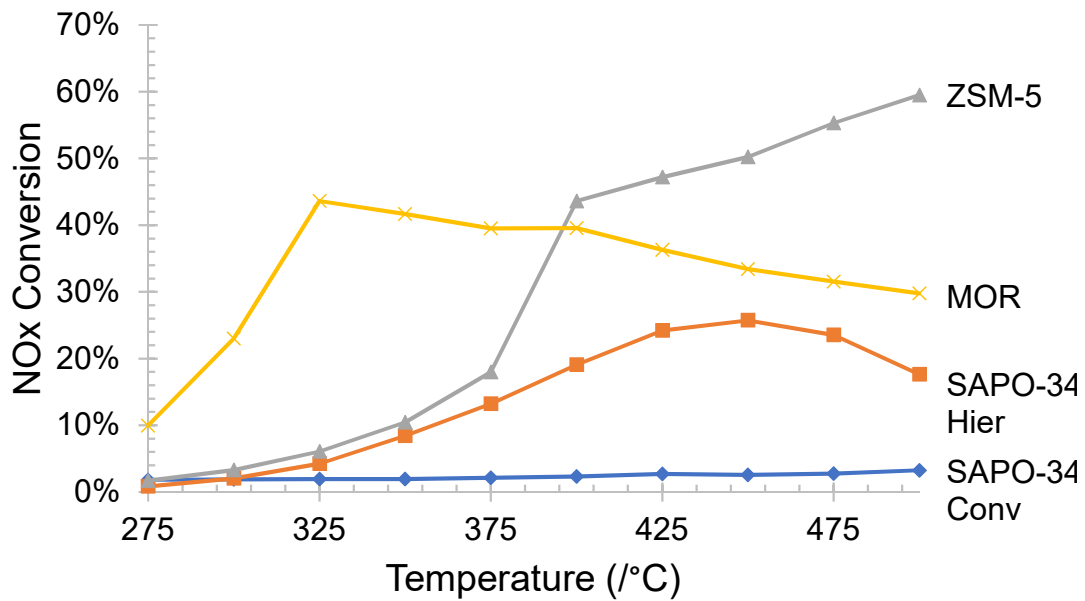
Figure 5-6: DeNOₓ results for [Ag+Cu]:Zeotypes. The same framework is used for the Ag:Z and Cu:Z in [Ag+Cu]:Z.

The high activity of [Ag+Cu]:ZSM-5 and [Ag+Cu]:MOR is also seen in Table 5-4. Interestingly, although [Ag+Cu]:ZSM-5 has the highest activity, [Ag+Cu]:MOR shows the largest activity window in that it is active between 325°C and 475°C inclusive. It must be noted that neither [Ag+Cu]:SAPO-34 Conv nor [Ag+Cu]:SAPO-34 Hier is considered active.

Table 5-4: Activity diagram for [Ag+Cu]:Zeotypes of the same zeotype.

Temperature (/°C)	275	300	325	350	375	400	425	450	475	500
SAPO-34 Conv										M
ZSM-5										M
MOR			M							
SAPO-34 Hier							M			

5.2.5 Summary of effect of mechanical mixing

As a whole, the results from the mechanically mixed samples with zeotype supported Ag and Cu suggest a notable negative effect of mechanical mixing compared to Cu:Z references. Although a reasonable activity is seen in the mechanical mixture of Ag in the large pore mordenite and Cu in the medium pore ZSM-5, the activity is still considerably lower than for the separate Cu:ZSM-5. Furthermore, [Ag+Cu]:MOR is seen to have the largest activity window of the mechanically mixed zeotypes, in that it is active between 325 and 475°C inclusive.

5.3 Catalysis - Effect of porosity

This section focuses on the effect porosity has on deNO$_x$ for the samples studied. As reference, the mechanically mixed [Ag+Cu]:Z is compared with the Ag:Z and Cu:Z reference samples, and the simultaneously ion exchanged AgCu:Z samples for each zeotype used. Notably, both [Ag+Cu]:Z and AgCu:Z samples contain Ag and Cu, but differ in preparation method. These samples are compared to elucidate if the conversion of the respective AgCu:Z and [Ag+Cu]:Z can be attributed to Cu:Z or Ag:Z; and what may be considered synergistic or destructive effects for each zeotype. Finally, deNO$_x$ results for AgCu:Z are compared for different zeotypes.

5.3.1   DeNOₓ results for ZSM-5 samples

Although the [Ag+Cu]:ZSM-5 activity has already been seen to be high, its conversion is surpassed by both AgCu:ZSM-5 and Cu:ZSM-5 as shown in Figure 5-7. Interestingly, the AgCu sample performs nearly equally to the Cu sample across the entire temperature range studied, in spite of the Ag content present in the AgCu sample.
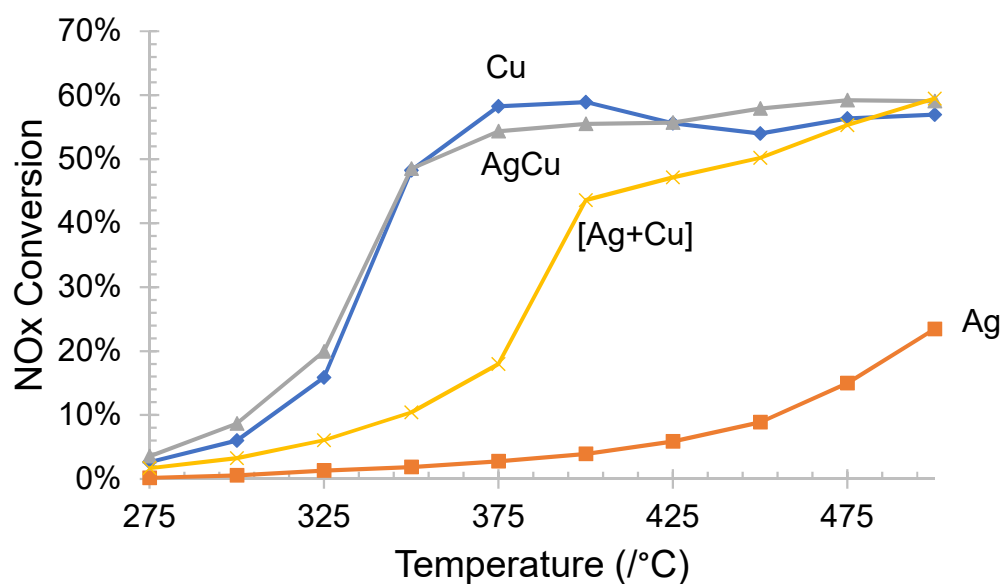
Figure 5-7: DeNOₓ results for ZSM-5 samples.

The high activity of ZSM-5 samples is also shown in Table 5-5, where all ZSM-5 samples but Ag are seen to be active from 400°C to 500°C inclusive. Additionally, the AgCu and Cu samples are also active at 350°C and 375°C. As a result, although [Ag+Cu]:ZSM-5 performs well with respect to other mechanically mixed samples, it still exhibits lower activity than its Cu:ZSM-5 reference sample.

Table 5-5: Activity diagram for ZSM-5 samples.

Temperature (/°C)	275	300	325	350	375	400	425	450	475	500
Ag										M
Cu					M					
[Ag+Cu]										M
AgCu									M	

39

5.3.2 DeNOₓ results for mordenite samples

With mordenite samples, [Ag+Cu]:MOR is seen to follow a similar trend of conversion as its Cu:MOR reference as shown in Figure 5-8. Notably, the order of conversion remains the same across the entire temperature range studied. In this respect, the Cu:MOR exhibits the highest conversion, similar to the results seen for the ZSM-5 samples.
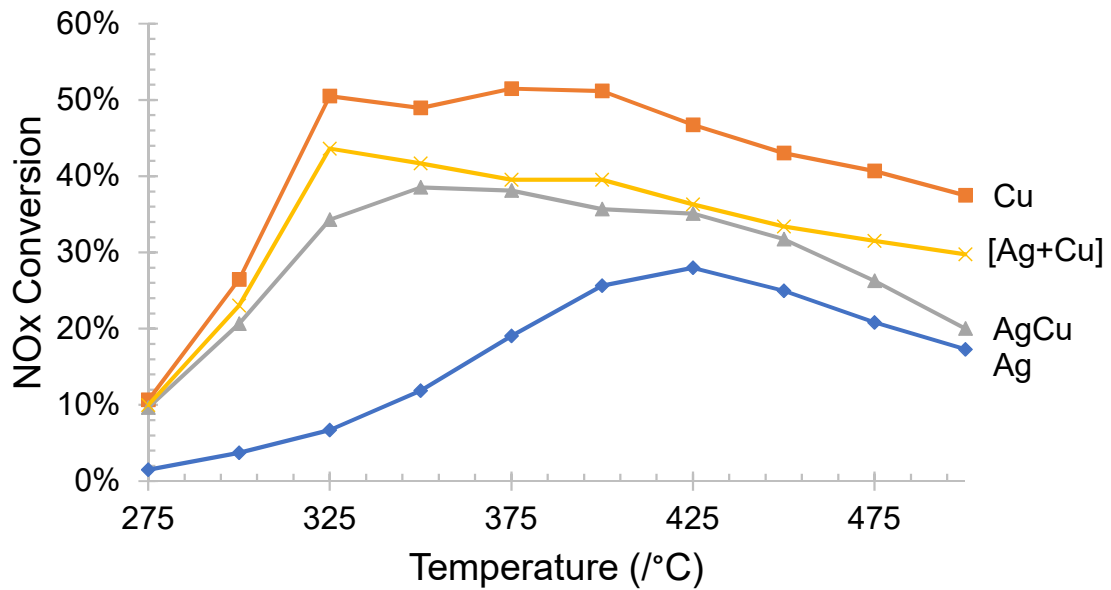
Figure 5-8: DeNOₓ results for mordenite samples.

The activity diagram in Table 5-6 also reflects the conversion declining in the order of Cu>[Ag+Cu]>AgCu>Ag. Among the mordenite samples, [Ag+Cu]:MOR shows the second largest activity window, close to the Cu:MOR reference sample.

Table 5-6: Activity diagram for mordenite samples.

Temperature (/°C)	275	300	325	350	375	400	425	450	475	500
Ag								M		
Cu						M				
[Ag+Cu]			M							
AgCu				M						

5.3.3 DeNOx results for SAPO-34 Hier samples

A more complex situation is seen for the hierarchical SAPO-34 samples in Figure 5-9 as the [Ag+Cu] catalyst performs best at temperatures above 425°C, though is surpassed by its Cu reference at lower temperatures. The Cu:SAPO-34 Hier reference has the highest conversion for these samples, with 32% conversion at 400°C.
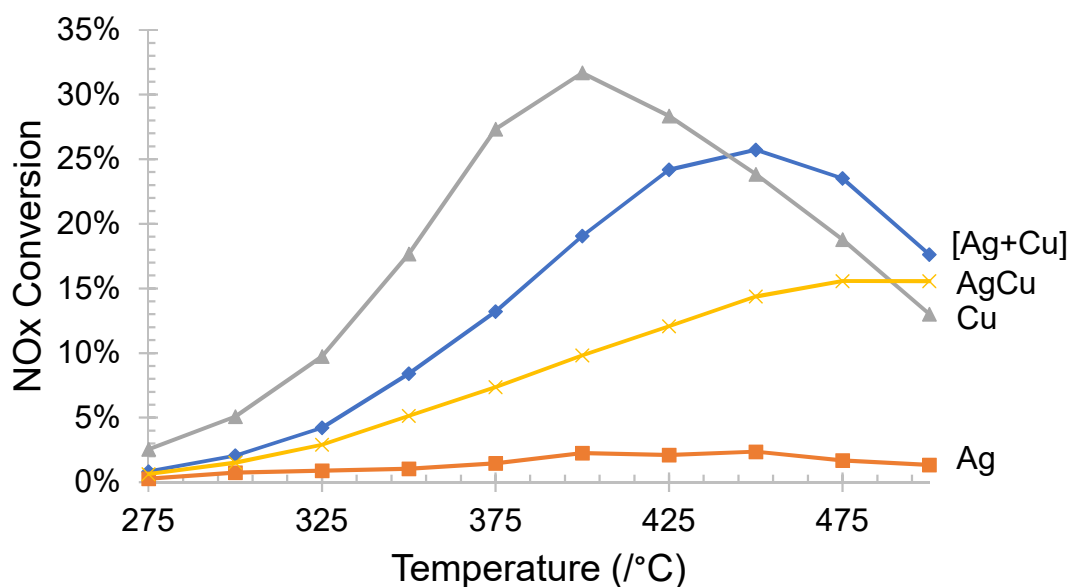
Figure 5-9: DeNO$_x$ for SAPO-34 Hier samples.

However, this peak conversion is also the only point at which the hierarchical SAPO-34 samples are active. This is seen in Table 5-7. The mechanically mixed [Ag+Cu] sample cannot be said to be active, similar to the Ag and AgCu samples.

Table 5-7: Activity diagram for SAPO-34 Hier samples.

Temperature (/°C)	275	300	325	350	375	400	425	450	475	500
Ag								M		
Cu						M				
[Ag+Cu]								M		
AgCu									M	

5.3.4 DeNO$_x$ results for SAPO-34 Conv samples

For the conventional SAPO-34 samples in Figure 5-10, no discernible activity is seen for neither the Ag reference sample, nor for the [Ag+Cu] sample. However, the AgCu sample is seen to surpass the Cu reference sample by nearly 20 percentage points at most. This suggests a synergistic effect of simultaneous ion exchange, at the same time as the low activity of mechanically mixed samples is reinforced.
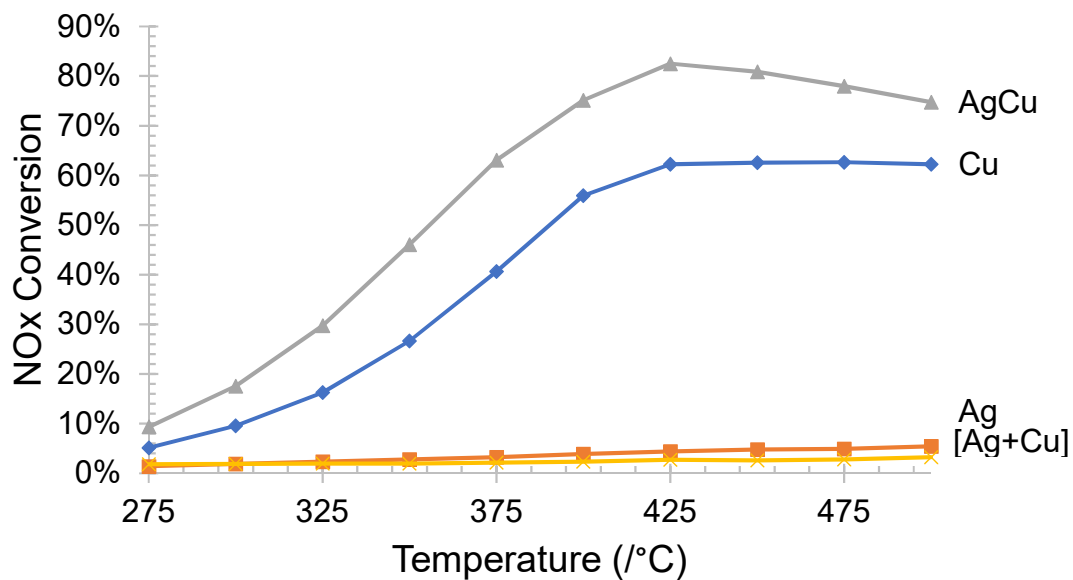
Figure 5-10: DeNO$_x$ for SAPO-34 Conv samples.

The AgCu sample also has the largest activity window as shown in Table 5-8, as it is active between 350°C and 500°C inclusive. As has already been seen, the [Ag+Cu] sample is not considered active.

Table 5-8: Activity diagram for SAPO-34 Conv samples.

Temperature (/°C)	275	300	325	350	375	400	425	450	475	500
Ag										M
Cu								M		
[Ag+Cu]										M
AgCu						M				

5.3.5 DeNOₓ results for AgCu:Zeotypes

5.3.5 DeNO$_x$ results for AgCu:Zeotypes

Finally, the deNO$_x$ results for the simultaneously ion exchanged AgCu samples are shown in Figure 5-11. The order of highest to lowest conversion correlates with pore size. In this sense, the small pore AgCu:SAPO-34 Conv sample shows the highest or close to highest conversion across the entire temperature range. Its peak conversion is 83% at 425°C, far above the next best sample, the medium pore ZSM-5, which shows a maximum conversion of 59% at 475°C. In addition to this, the AgCu:SAPO-34 sample has the highest deNO$_x$ conversion of all samples tested.
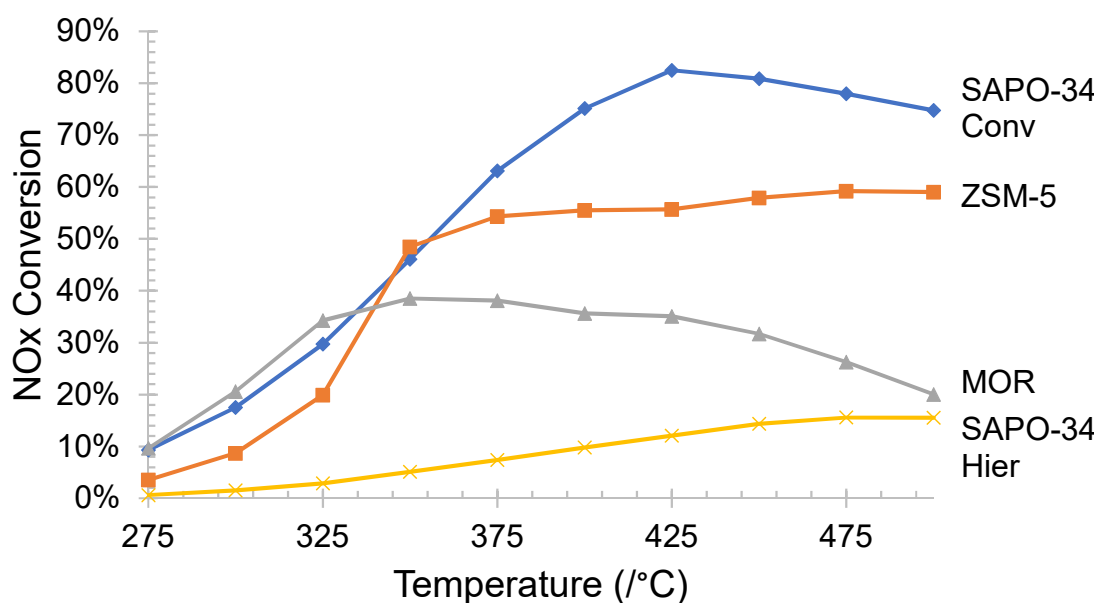
Figure 5-11: DeNO$_x$ results for AgCu:Zeotypes.

With respect to activities shown in Table 5-9, both ZSM-5 and SAPO-34 Conv have equally wide activity windows as they are active from 350°C and onwards. Notably, the SAPO-34 Hier sample is not active.

Table 5-9: Activity diagram for AgCu:Zeotype samples.

Temperature (/°C)	275	300	325	350	375	400	425	450	475	500
SAPO-34 Conv							M			
ZSM-5									M	
MOR				M						
SAPO-34 Hier									M	

5.3.6 Summary of effect of porosity

With respect to the above section, the small pore AgCu samples exhibit the highest activity of all studied samples. The activities of the AgCu samples also appear to correlate inversely with pore size; as the activity is in the order of SAPO-34 Conv>ZSM-5>MOR>SAPO-34 Hier; from small pores to mesopores. Conversely, [Ag+Cu]:Z samples tend to have an intermediate or no activity, whereas the AgCu:Z samples have intermediate or high $deNO_x$ conversions.

6.0 Discussion

In this master's thesis, the effect of mechanical mixing and porosity on the activity of Ag and Cu ion exchanged zeotypes has been investigated in the HC-SCR of NO_x. As the dual pore concept is thought to increase the NO_x conversion relative to its components, [Ag+Cu]:Z and AgCu:Z samples have been catalytically tested and compared to Ag:Z and Cu:Z reference samples.[3, 10] This discussion aims to rationalize these results, and to demonstrate the connection between the results and current research. A complete comparison of catalyst activities is found in Appendix D: Complete activity diagram for all samples studied.

6.1 Effect of mechanical mixing

Mechanically mixed Ag:Z and Cu:Z catalysts studied in this thesis show a negative effect of mechanical mixing on NO_x conversion. In particular, Table 6-1 shows how separate Cu:Z catalysts perform better than all mechanically mixed [Ag+Cu]:Z catalysts at 425°C. The catalysts are compared at 425°C as the intermediate activity of mechanically mixed catalysts is clearly shown at this temperature. The results of mechanically mixed catalysts may be further divided into two groups: dual pore systems and mechanically mixed zeotypes of the same framework.

Table 6-1: DeNO$_x$ conversion at 425°C for [Ag+Cu]:Z and Cu:Z catalysts with respect to the pore sizes in which Ag and Cu are located. Results from [Ag+Cu]:Z are used for equal pore sizes. Bold indicates the highest conversion for each Cu pore size. Within each category, green indicates higher values, whereas blue indicates lower values.

			Ag position			
		Cu reference	Small	Medium	Large	Meso+ small
Cu position	Small	62 %	3 %	8 %		37 %
	Medium	56 %		47 %	39 %	
	Large	47 %		3 %	36 %	
	Meso+ Small	28 %				24 %

For dual pore systems, the Ag:Z and Cu:Z used in the mechanically mixed catalyst are present in different zeotypes. By containing the oxidative function, in this case Cu, in small pores, bulkier hydrocarbons are thought to be restricted entry.[3, 10] However, this is not thought to be the case for the dual pore systems considered in this thesis. With respect to Table 6-1, the highest dual pore activity for Cu in the small pore SAPO-34 is 37% at 425°C. This is considerably lower than the separate reference Cu:SAPO-34, with 62% conversion at 425°C. These results also hold for all other dual pore systems studied; the Cu:Z reference performs better than mechanically mixed catalysts with dual pore systems. This conflicts with the theory on the dual pore concept. In other words, for the samples studied in this thesis, dual pore systems yield a negative effect on NO_x conversion.

Mechanical mixing of Ag:Z and Cu:Z in the same zeotype means both the oxidative and reductive functions will be subject to the same size restrictions. A synergistic effect of this mixing is not seen, which is attributed to the separation of the catalytic functions. These results are presented in Table 6-1. This case also speaks against having Cu in small pores; indeed, the sample with Ag and Cu in the small pore SAPO-34 Conv has the lowest conversion at 425°C, with only 3% NO_x conversion. The low activities of the small pore mechanically mixed catalyst are inconsistent with theory, where it is thought that having Cu in smaller pores would yield increased NO_x conversion due to shape selective restriction.[3, 10] Notably, the highest conversion for these mechanically mixed catalysts is seen for Ag and Cu in the medium pore ZSM-5, with 47% NO_x conversion at 425°C. Despite the low conversion of the mechanically mixed small pore catalysts, propene is not thought to be shape selectively restricted access into the small pores of SAPO-34 Conv as the small pore Cu reference sample has 62 % conversion at 425°C, higher still than the best mechanically mixed catalyst. A lower activity of the Cu reference sample is expected if propene were restricted entry into the small pore SAPO-34 Conv.

Put short, for the samples studied, a notable decrease in NO_x conversion is seen for mechanically mixed catalysts with Ag:Z and Cu:Z compared to the separate Cu:Z used. This is the case both for dual pore system catalysts and mechanically mixed catalysts using the same zeotype. In turn, this suggests that the dual pore concept does not work.

6.2 Effect of zeotype porosity

The effect porosity has on deNO$_x$ conversion is considered in this part, with particular focus on the AgCu:Z catalysts, and the differences between the [Ag+Cu]:Z and AgCu:Z catalysts.

A trend of increasing NO$_x$ conversion is seen for smaller pore sizes for the simultaneously ion exchanged AgCu:Z. This is shown in Table 6-2, where the AgCu sample with the small pore SAPO-34 Conv has the highest deNO$_x$ conversion with 83% at 425°C compared to only 3% for [Ag+Cu] in SAPO-34 Conv. Furthermore, the results of AgCu:Z surpass those of Cu:Z for small and medium pore sizes. These results, in turn, suggest a synergistic effect of simultaneous ion exchange of Ag and Cu compared to mechanically mixed catalysts, which is most substantial with small pores. As a result, the differences in deNO$_x$ conversions between [Ag+Cu]:Z and AgCu:Z catalysts may be explained by diffusion or the local coordination of Ag and Cu in the two sets of catalysts.

Table 6-2: DeNO$_x$ conversion at 425°C with respect to the pore sizes in which Ag and Cu are located. Results from AgCu:Z are used for equal pore sizes. Bold indicates the highest conversion for each Cu pore size. Within each category, green indicates higher values, whereas blue indicates lower values.

		Cu reference	Small	Ag position Medium	Large	Meso+ small
	Small	62 %	**83 %**	8 %		37 %
	Medium	56 %		**56 %**	39 %	
Cu position	**Large**	47 %		3 %	35 %	
	Meso+ Small	28 %				12 %

Diffusion caused by different porosities may explain the differences between the AgCu:Z and [Ag+Cu]:Z sample activities. As has been pointed out earlier, propene is not thought to be restricted entry into the small pore SAPO-34 Conv by shape selectivity. Additionally, the effect of mechanical mixing was originally thought to be enhanced by using dual pore systems; where Ag:Z and Cu:Z are in different zeotypes, though this appears not to be the case. A possibility is if the dual pore concept does not work as intended. In [Ag+Cu] catalysts, the oxidative and reductive functions are present in separate Ag and Cu crystallites as a result of mechanical mixing of Ag:Z and Cu:Z references. If NO$_2$ is generated at the oxidative function in the

[Ag+Cu] catalyst before diffusing into the reductive function, the increased time of diffusion may allow the hydrocarbon to be oxidized directly. This would explain how the highest [Ag+Cu]:Z activity is seen for the medium pore ZSM-5; for large pores and mesopores, the oxidative function may be too accessible for propene, thereby allowing direct oxidation. In other words, as the effect of shape selectivity is reduced with increased pore sizes, propene may diffuse and react freely.[48] For the small pore SAPO-34 Conv, however, the diffusion between crystallites may simply be too slow to allow HC-SCR of NO_x to take place appreciably in mechanically mixed samples. By comparison, with AgCu in small pores, both the reductive and oxidative functions of Ag and Cu respectively are present in the same crystallites, which in turn would necessitate less diffusion. The direct oxidation of the hydrocarbon within large pores and mesopores may still be the case; however, in small pores, no additional diffusion is required for NO_2 to be reduced by the hydrocarbon after NO_2 has been generated. Hence, the differences between the AgCu:Z and [Ag+Cu]:Z catalysts' performance may be rationalized by differences in diffusion, as less diffusion is thought to be necessary in AgCu:Z catalysts.

Diffusional limitation caused by small pores is contested by research on ammonium-SCR with Cu:Z in small pores, which suggests that pore diffusion is not the most important factor for the reaction rate, but rather kinetic control.[74] On the other hand, one of the suggested reaction mechanisms for HC-SCR involve the generation of an organonitric compound which in turn reacts with water to form ammonium.[57] In this regard, diffusion rate is likely to play a larger role in HC-SCR than ammonium-SCR. This is because the hydrocarbon must react with NO_x on a catalytic centre before ammonium is formed in HC-SCR, steps which are not relevant in ammonium-SCR due to the presence of NH_3.[55, 57]

Moreover, in AgCu:Z, the presence of both Ag and Cu may have lead each metal to assume less common positions in the zeotype compared to a singly ion exchanged zeotype.[69] In turn, local coordination can influence the availability of the catalytic functions in zeotypes. Indeed, as seen before, the Cu positions in zeotypes are influenced by simultaneous ion exchange.[69] This idea is supported by the differences in activity between [Ag+Cu]:Z and AgCu:Z in small and medium pore systems. Studying the outputs of AgCu:Z and Cu:Z by GCMS may reveal more about these differences. Further research is also required to determine the specific local environment of Ag and Cu for different samples.

A combination of the effects of diffusion and differences in local metal coordination is thought to rationalize the trend of higher deNO$_x$ conversion for smaller pore zeotypes for AgCu:Z catalysts than for [Ag+Cu]:Z catalysts.

The effect of porosity and metal position on deNO$_x$ conversion is also seen in the considerable differences between mechanically mixed catalysts with Ag in medium pores and Cu in large pores compared to the opposite. As seen in Table 6-1, the latter has a NO$_x$ conversion of 39% at 425°C, the former has only 3% NO$_x$ conversion at this temperature. Despite this, the activity does not exceed that of the separate Cu:Z catalysts. One theory on the dual pore system suggested having the reductive function in large pores and oxidative function in small pores.[3] In this work, that corresponds to having Ag in large pores and Cu in small pores; thereby separating the reductive and oxidative functions.[3] In this regard, employing the dual pore concept does not appear to increase deNO$_x$ conversion beyond that of singly ion exchanged catalysts. It should be noted that the conversion of mechanically mixed samples in the presence of water and SO$_2$ has not been studied. Considering the deactivation shown in the presence of water with Cu in medium size pores, mechanically mixed catalysts may perform better by comparison in the presence of these poisons.[7] Nevertheless, under dry conditions, although porosity and position of metal is seen to influence the deNO$_x$ conversion of mechanically mixed catalysts, the effect is still negative compared to the Cu reference samples.

Larger pores reduce diffusion limitations, and thereby increase the efficiency of the micropores.[4] However, the mesoporous SAPO-34 Hier confers no increased deNO$_x$ activity compared to the small pore SAPO-34 Conv with the sole exception of [Ag+Cu]:SAPO-34 Hier. In all other categories, SAPO-34 Hier has the lowest activity. Following the above rationale, SAPO-34 Hier may be worse off than SAPO-34 Conv, as large pores and high diffusion is thought to increase hydrocarbon direct oxidation.[10] Thereby, it may jeopardize the intended effect of separating the oxidative and reductive functions of the catalyst.[10] Another reason could be hydrothermal structural collapse during ion exchange; SAPO-34 Hier is seen to be less crystalline than SAPO-34 Conv.[70]

In total, a synergistic effect on NO$_x$ conversion is observed for AgCu:Z, which becomes enhanced with small and medium pore zeotypes like SAPO-34 Conv and ZSM-5 respectively. The high activity of these samples is contrasted by the low activities of mechanically mixed samples. These dissimilarities may be rationalized by differences in diffusion and local coordination of metals; more diffusion between crystallites is thought necessary in

mechanically mixed catalysts than in simultaneously ion exchanged catalysts. In mechanical mixing, vastly different results for are seen for Ag and Cu in different pore sizes, though these results do not surpass the conversion of the separate Cu:Z samples. Finally, the mesoporous SAPO-34 Hier has very low conversion across the samples tested. This may be caused by framework collapse during ion exchange, or that the mesopores render direct oxidation of the hydrocarbon more available.

6.3 Effect of metal content

Differences in metal content are not thought to be a significant factor for deNO$_x$ activity above a certain metal content. For instance, [Ag+Cu]:Z for small pores contains 2 wt% each of Ag and Cu, compared to 8 and 5 wt% respectively for AgCu:Z. This is seen in Table 6-3. The metal content is not thought important, mainly due to the inactivity of the [Ag+Cu] catalyst for small pores. Increased metal content is not thought to make the activity of the [Ag+Cu] comparable to the AgCu catalyst for the small pore SAPO-34 Conv. However, in the medium pore ZSM-5 system, though the AgCu catalyst contains only half the Cu content of Cu catalyst, these catalysts perform nearly identically across the temperature range. This is in line with research by Chajar, et al. [7]; where it was seen that as the Cu content becomes greater than 1 wt%, the medium pore AgCu:ZSM-5 zeotype behaves similar to Cu:Z, even with additional silver content. This theory is further supported as [Ag+Cu]:Z in large and mesopores have a higher maximum conversion than do AgCu:Z despite containing less metal. In a similar case, a paper which considers alumina supported potassium-copper and potassium-cobalt catalysts for deNO$_x$ and particulate removal found highest NO conversion activity for the catalyst with the highest metal content.[75] Put short, differences in metal content in the tested samples are not thought to be a significant factor for the differences in deNO$_x$ activities.

The resulting metal contents for the simultaneously exchanged AgCu:Z are not comparable to the work done on Zeolite Y.[69] With Zeolite Y, a 1:1 wt% relationship of Ag:Cu was achieved when the solution used for ion exchange contained a 4:1 ratio of Ag:Cu by mass.[69] The varying metal content of the AgCu:Z samples can be seen in Table 6-3. Specifically, it appears MOR has a particular affinity for accepting Ag during ion exchange. It may also be noted how the Cu content of AgCu:Z varies, its range is from 2 to 5 wt%, compared to 6 to 12 wt% for Ag.

Table 6-3: Maximum NO$_x$ conversion, temperature of maximum NO$_x$ conversion and metal content of [Ag+Cu]:Z and AgCu:Z samples. Within each category, green indicates higher values, whereas blue indicates lower values.

Pore size	[Ag+Cu]				AgCu			
	Conv$_{max}$	T$_{maxconv}$ (/°C)	Ag (/Wt%)	Cu (/Wt%)	Conv$_{max}$	T$_{maxconv}$ (/°C)	Ag (/Wt%)	Cu (/Wt%)
Small	3 %	500	2 %	2 %	83 %	425	8 %	5 %
Medium	59 %	500	2 %	2 %	59 %	475	8 %	2 %
Large	44 %	325	4 %	3 %	39 %	350	12 %	3 %
Meso	26 %	450	1 %	3 %	16 %	475	6 %	4 %

6.4 Candidate for future catalysis

The studied AgCu:SAPO-34 Conv sample is the most promising sample for future catalysis. This sample has a higher total metal loading, 83% peak conversion and 20 percentage points increased deNO$_x$ conversion compared to Cu:SAPO-34 Conv at higher temperatures. In a recent review by Mrad, et al. [29], the activities of several HC-SCR catalysts have been compared. The Cu catalysts presented here have NO conversions of 40 and 20%.[29] Conversions as high as 74% have also been seen with a ZSM-5 catalyst containing Ag and Cu.[7] Work presented in this thesis shows how the small pore Cu:SAPO-34 Conv has a maximum conversion of 63%. Compared to these samples, the AgCu:SAPO-34 Conv catalyst prepared can be said to have very high conversion compared to related catalysts. The catalyst is active between 350°C and 500°C inclusive, and conversion is above 60% between 375°C and 500°C inclusive. This renders the simultaneously ion exchanged AgCu:SAPO-34 Conv a prime candidate for future catalytic testing. Although the future applicability of this catalyst is dependent upon its N$_2$ selectivity and activities in realistic conditions with water and SO$_2$, the high maximum activity and large activity window shows great promise for use in future deNO$_x$ catalysis.

7.0   Conclusion

Mechanically mixed [Ag+Cu]:Zeotypes yield a negative effect on activity compared to the respective Cu:Zeotype in the case of MOR, ZSM-5 and SAPO-34 Conv. This is also the case for SAPO-34 Hier below 450°C. Physical separation and diffusion between crystallites may be part of the explanation for the low activities. As such, the dual pore concept is not seen to improve activities under the studied conditions. The dissimilarities between AgCu:Zeotypes and [Ag+Cu]:Zeotypes is attributed to differences in diffusion and local coordination of Ag and Cu.

Simultaneous ion exchange with Ag and Cu show a synergistic effect of smaller pores for the deNO$_x$ activity. The small pore AgCu:SAPO-34 Conv has been found to yield a peak deNO$_x$ activity of 83%, and a higher total metal loading compared to Cu:SAPO-34 Conv. This is the best performing of the investigated zeotypes, and is 20 percentage points higher than Cu:SAPO-34 Conv. It is also very high compared to related metal exchanged zeotypes, however the reaction products must be analysed. Metal loading does not appear to be the only factor at play. The reason for the high activity is thought to be differences in local coordination between Cu:SAPO-34 Conv and AgCu:SAPO-34 Conv combined with an enhanced effect of the small pore system.

The mesoporous SAPO-34 Hier zeotype confers no increased deNO$_x$ activity compared to SAPO-34 Conv save [Ag+Cu]:SAPO-34 Hier. In all other categories, SAPO-34 Hier has the lowest activity of the investigated zeotypes. It is thought to be caused by high direct oxidation of propene, due to the increased theoretical availability of catalytic centres resulting from mesopore, in addition to structural collapse during ion exchange.

Simultaneous ion exchange with Ag and Cu appears not to give consistent metal contents in MOR, ZSM-5, SAPO-34 Conv and SAPO-34 Hier samples when using a 4:1 mass relationship of Ag to Cu in the employed solutions for ion exchange. These samples, however, display an increased total metal content compared to Ag:Z and Cu:Z combined.

8.0   Future work

With respect to the presented work, several topics could use further investigation. Firstly, the AgCu:SAPO-34 Conv catalyst should be tested under realistic conditions; that is, the effect of water and SO_2 should be tested. The lifetime of the catalyst must also be investigated. This could determine whether the most active catalyst identified in this thesis is applicable for its intended use in small vehicles. The dual pore concept could also be studied further under these conditions. The effect of varying hydrocarbons should also be determined. Also relevant to the potential real-life application of the AgCu:SAPO-34 Conv catalyst is what is produced during catalysis; what part NO_x is converted to N_2, and what organic species result from catalytic conversion.

It has been seen that AgCu:Z and [Ag+Cu]:Z have yielded different results, even in the cases where metal contents have been similar. By investigating the position of metal atoms in the different structures after ion exchange, the nature of this effect may be deduced.

Mechanically mixed zeotypes have shown different activities to their non-mixed counterparts. This has, however, only been considered for 1:1 mixtures of Ag:Z and Cu:Z. The effect of different mixing ratios has not been considered, and may benefit from further study.

Further investigation may also be done on the two-cation effect on ion exchange. In the present work, the metal contents of AgCu:Z and [Ag+Cu]:Z have not been consistently comparable. By looking closer at the link between ion exchange solution and resulting metal content, the effect of different metal loading between samples may be reduced when comparing samples.

9.0   References

1.   Baerlocher, C.; McCusker, L. B., Database of Zeolite Structures: http://www.iza-structure.org/databases/.
2.   Ministry of Climate and Environment Nitrogenoksid (NOx). http://www.miljostatus.no/Tema/Luftforurensning/Sur-nedbor/Nitrogenoksid-NOx.
3.   Brosius, R.; Martens, J. A., Reaction Mechanisms of Lean-Burn Hydrocarbon SCR over Zeolite Catalysts. *Topics in Catalysis* **2004,** *28* (1), 119-130.
4.   Perez-Ramirez, J.; Christensen, C. H.; Egeblad, K.; Christensen, C. H.; Groen, J. C., Hierarchical zeolites: enhanced utilisation of microporous crystals in catalysis by advances in materials design. *Chemical Society Reviews* **2008,** *37* (11), 2530-2542.
5.   Safi, M. India to introduce clean fuels faster to combat Delhi smog crisis. https://www.theguardian.com/world/2017/nov/15/india-to-introduce-clean-fuels-faster-to-combat-delhi-smog-crisis (accessed 28. Nov).
6.   William D. Callister, J.; Rethwisch, D. G., Costs and Relative Costs for Selected Engineering Materials. In *Materials Science and Engineering*, John Wiley & sons: 2015; pp 857-861.
7.   Chajar, Z.; Denton, P.; Berthet de Bernard, F.; Primet, M.; Praliaud, H., Influence of silver on the catalytic activity of Cu-ZSM-5 for NO SCR by propane. Effect of the presence of water and hydrothermal agings. *Catalysis Letters* **1998,** *55* (3), 217-222.
8.   Masuda, K.; Shinoda, K.; Kato, T.; Tsujimura, K., Activity enhancement of Ag/mordenite catalysts by addition of palladium for the removal of nitrogen oxides from diesel engine exhaust gas. *Applied Catalysis B: Environmental* **1998,** *15* (1), 29-35.
9.   Holma, T.; Palmqvist, A.; Skoglundh, M.; Jobson, E., Continuous lean NOx reduction with hydrocarbons over dual pore system catalysts. *Applied Catalysis B: Environmental* **2004,** *48* (2), 95-100.
10.   Martens, J. A.; Cauvel, A.; Jayat, F.; Vergne, S.; Jobson, E., Molecule sieving catalysts for NO reduction with hydrocarbons in exhaust of lean burn gasoline and diesel engines. *Applied Catalysis B: Environmental* **2001,** *29* (4), 299-306.
11.   Ministry of Climate and Environment Veitrafikk og luftforurensning. http://www.miljostatus.no/tema/luftforurensning/utslipp-fra-veitrafikk/.
12.   Fontaínhas, J.; Cunha, J.; Ferreira, P., Is investing in an electric car worthwhile from a consumers' perspective? *Energy* **2016,** *115* (Part 2), 1459-1477.
13.   Propfe, B.; Kreyenberg, D.; Wind, J.; Schmid, S., Market penetration analysis of electric vehicles in the German passenger car market towards 2030. *International Journal of Hydrogen Energy* **2013,** *38* (13), 5201-5208.
14.   Kihm, A.; Trommer, S., The new car market for electric vehicles and the potential for fuel substitution. *Energy Policy* **2014,** *73* (Supplement C), 147-157.
15.   Hromádko, J.; Miler, P.; Hromádko, J.; Hönig, V.; Schwarzkopf, M., The influence of three-way catalysts on harmful emission production. *Transportation Research Part D: Transport and Environment* **2010,** *15* (2), 103-107.
16.   Shelef, M., Selective Catalytic Reduction of NOx with N-Free Reductants. *Chemical Reviews* **1995,** *95* (1), 209-225.
17.   Wayne, R. P., *Chemistry of atmospheres, third edition*. Oxford University Press: 2000.
18.   Santhosham, A.; Aghalayam, P., Understanding NO emissions in diesel and biodiesel based engines. *RSC Advances* **2016,** *6* (64), 59513-59526.
19.   Pedersen, B. NOx. https://snl.no/NOx.
20.   Nestaas, I.; Brænd, T. J.; Olerud, K. Sur Nedbør. https://snl.no/sur_nedb%C3%B8r.
21.   Skoog, D. A.; West, D. M.; Holler, F. J.; Crouch, S. R., Aqueous Solutions and Chemical Equilibria. In *Fundamentals of analytical Chemistry*, Cengage Learning: 2014; pp 227-231.
22.   United Nations GHG data from UNFCCC. http://unfccc.int/ghg_data/ghg_data_unfccc/items/4146.php (accessed 20. Aug).

23.   United Nations, Kyoto Protocol to the United Nations Framework Convention on Climate Change. 1997.

24.   European Environment Agency *Air Quality in Europe - 2016 report*; European Environment Agency: Luxembourg, 2016.

25.   Pârvulescu, V. I.; Grange, P.; Delmon, B., Catalytic removal of NO. *Catalysis Today* **1998,** *46* (4), 233-316.

26.   Ogidiama, O. V.; Shamim, T., Performance Analysis of Industrial Selective Catalytic Reduction (SCR) Systems. *Energy Procedia* **2014,** *61*, 2154-2157.

27.   Held, W.; König, A.; Richter, T.; Puppe, L., Catalytic NOx Reduction in Net Oxidizing Exhaust Gas. SAE International: 1990.

28.   Iwamoto, M.; Yahiro, H.; Yu-u, Y.; Shundo, S.; Mizuno, N., Selective reduction of NO by lower hydrocarbons in the presence of O2 and SO2 over copper ion-exchanged zeolites. *Shokubai (catalyst)* **1990,** *32* (6), 430-433.

29.   Mrad, R.; Aissat, A.; Cousin, R.; Courcot, D.; Siffert, S., Catalysts for NOx selective catalytic reduction by hydrocarbons (HC-SCR). *Applied Catalysis A: General* **2015,** *504*, 542-548.

30.   Iwamoto, M.; Yahiro, H.; Shundo, S.; Yu-u, Y.; Mizuno, N., Influence of sulfur dioxide on catalytic removal of nitric oxide over copper ion-exchanged ZSM-5 zeolite. *Applied Catalysis* **1991,** *69* (1), L15-L19.

31.   Torre-Abreu, C.; Henriques, C.; Ribeiro, F. R.; Delahay, G.; Ribeiro, M. F., Selective catalytic reduction of NO on copper-exchanged zeolites: the role of the structure of the zeolite in the nature of copper-active sites. *Catalysis Today* **1999,** *54* (4), 407-418.

32.   Chen, H.-Y.; Wang, X.; Sachtler, W. M. H., Reduction of NOx over various Fe/zeolite catalysts. *Applied Catalysis A: General* **2000,** *194*, 159-168.

33.   European Environment Agency Emissions of the main air pollutants in Europe. https://www.eea.europa.eu/data-and-maps/indicators/main-anthropogenic-air-pollutant-emissions/assessment-5 (accessed 20. Aug).

34.   Manahan, S. E., Photochemical Smog. In *Environmental Chemistry*, 9th ed.; CRC Press: 2010.

35.   European Environment Agency Comparison of NOx emission standards for different Euro classes. https://www.eea.europa.eu/media/infographics/comparison-of-nox-emission-standards/view (accessed 20. Aug).

36.   Folkehelseinstituttet *Luftkvalitetskriterier - Virkninger av luftforurensning på helse*; 2013; pp 65-79.

37.   Hotten, R., Volkswagen: The scandal explained. *BBC News* 10.12.2015, 2015.

38.   Silman, S., Tropospheric Ozone and Photochemical Smog. In *Environmental Geochemistry*, Lollar, B. S., Ed. Elsevier: 2005; Vol. 9.

39.   Opdahl, H.; Arnesen, H. nitrogenmonoksid. https://sml.snl.no/nitrogenmonoksid.

40.   Zumdahl, S. S., Gases. In *Chemical principles*, Houghton Mifflin: 1998; pp 172-175.

41.   Nestaas, I. Fotokjemisk Smog. https://snl.no/fotokjemisk_smog (accessed 24. Oct).

42.   Liu, Z.; Ihl Woo, S., Recent Advances in Catalytic DeNOX Science and Technology. *Catalysis Reviews* **2006,** *48* (1), 43-89.

43.   Zeolites. In *Springer Handbook of Nanomaterials*, Vajtai, R., Ed. Springer: Berlin, Heidelberg, 2013; pp 819-857.

44.   Jha, B.; Singh, D. N., Basics of Zeolites. In *Fly Ash Zeolites: Innovations, Applications, and Directions*, Springer Singapore: Singapore, 2016; pp 5-31.

45.   Science and Engineering of Nanomaterials. In *Springer Handbook of Nanomaterials*, Vajtai, R., Ed. Springer: Berlin, Heidelberg, 2013; pp 1-31.

46.   Maschmeyer, T.; van de water, L., *An Overview of Zeolite, Zeotype and Mesoporous Solids Chemistry: Design, Synthesis and Catalytic Properties*. 2006; Vol. 4, p 1-38.

47.   Webster, C. E.; Drago, R. S.; Zerner, M. C., A Method for Characterizing Effective Pore Sizes of Catalysts. *The Journal of Physical Chemistry B* **1999,** *103* (8), 1242-1249.

48.   Derouane, E. G.; Dejaifve, P.; Gabelica, Z.; Vedrine, J. C., Molecular shape selectivity of ZSM-5, modified ZSM-5 and ZSM-11 type zeolites. *Faraday Discussions of the Chemical Society* **1981,** *72* (0), 331-344.

49.   Feliczak-Guzik, A., Hierarchical zeolites: Synthesis and catalytic properties. *Microporous and Mesoporous Materials* **2017**.

50.   Azizi, Y.; Kambolis, A.; Boréave, A.; Giroir-Fendler, A.; Retailleau-Mevel, L.; Guiot, B.; Marchand, O.; Walter, M.; Desse, M. L.; Marchin, L.; Vernoux, P., NOx abatement in the exhaust of lean-burn natural gas engines over Ag-supported γ-Al2O3 catalysts. *Surface Science* **2016,** *646* (Supplement C), 186-193.

51.   Qi, G.; Yang, R. T., Low-temperature selective catalytic reduction of NO with NH3 over iron and manganese oxides supported on titania. *Applied Catalysis B: Environmental* **2003,** *44* (3), 217-225.

52.   German Association of the Automotive Industry AdBlue®. https://www.vda.de/en/topics/innovation-and-technology/ad-blue/AdBlue-brand-list-and-licensees-list.html.

53.   Miyadera, T., Selective reduction of nitric oxide with ethanol over an alumina-supported silver catalyst. *Applied Catalysis B: Environmental* **1997,** *13* (2), 157-165.

54.   Mathisen, K.; Nicholson, D. G.; Beale, A. M.; Sanchez-Sanchez, M.; Sankar, G.; Bras, W.; Nikitenko, S., Comparing CuAPO-5 with Cu:ZSM-5 in the Selective Catalytic Reduction of NOx: An in situ Study. *The Journal of Physical Chemistry C* **2007,** *111* (7), 3130-3138.

55.   Moreno-González, M.; Palomares, A. E.; Chiesa, M.; Boronat, M.; Giamello, E.; Blasco, T., Evidence of a Cu2+−Alkane Interaction in Cu-Zeolite Catalysts Crucial for the Selective Catalytic Reduction of NOx with Hydrocarbons. *ACS Catalysis* **2017,** *7* (5), 3501-3509.

56.   Gorce, O.; Baudin, F.; Thomas, C.; Da Costa, P.; Djéga-Mariadassou, G., On the role of organic nitrogen-containing species as intermediates in the hydrocarbon-assisted SCR of NOx. *Applied Catalysis B: Environmental* **2004,** *54* (2), 69-84.

57.   Li, L.; Guan, N., HC-SCR reaction pathways on ion exchanged ZSM-5 catalysts. *Microporous and Mesoporous Materials* **2009,** *117* (1), 450-457.

58.   Blakeman, P. G.; Burkholder, E. M.; Chen, H.-Y.; Collier, J. E.; Fedeyko, J. M.; Jobson, H.; Rajaram, R. R., The role of pore size on the thermal stability of zeolite supported Cu SCR catalysts. *Catalysis Today* **2014,** *231*, 56-63.

59.   Bethke, K. A.; H. Kung, H., *Supported Ag Catalysts for the Lean Reduction of NO with C 3H 6*. 1997; Vol. 172, p 93-102.

60.   Seijger, G. B. F.; van Kooten Niekerk, P.; Krishna, K.; Calis, H. P. A.; van Bekkum, H.; van den Bleek, C. M., Screening of silver and cerium exchanged zeolite catalysts for the lean burn reduction of NOx with propene. *Applied Catalysis B: Environmental* **2003,** *40* (1), 31-42.

61.   Boutros, M.; Trichard, J.-M.; Da Costa, P., Silver supported mesoporous SBA-15 as potential catalysts for SCR NOx by ethanol. *Applied Catalysis B: Environmental* **2009,** *91* (3), 640-648.

62.   Mathisen, K.; Nilsen, M. H.; Nordhei, C.; Nicholson, D. G., Irreversible Silver(I) Interconversion in Ag:ZSM-5 and Ag:SAPO-5 by Propene and Hydrogen. *The Journal of Physical Chemistry C* **2012,** *116* (1), 171-184.

63.   Shimizu, K.-i.; Satsuma, A., Selective catalytic reduction of NO over supported silver catalysts-practical and mechanistic aspects. *Physical Chemistry Chemical Physics* **2006,** *8* (23), 2677-2695.

64.   Shibata, J.; Takada, Y.; Shichi, A.; Satokawa, S.; Satsuma, A.; Hattori, T., Influence of zeolite support on activity enhancement by addition of hydrogen for SCR of NO by propane over Ag-zeolites. *Applied Catalysis B: Environmental* **2004,** *54* (3), 137-144.

65.   Ukisu, Y.; Miyadera, T.; Abe, A.; Yoshida, K., Infrared study of catalytic reduction of lean NOx with alcohols over alumina-supported silver catalyst. *Catalysis Letters* **1996,** *39* (3), 265-267.

66.   Leistner, K.; Mihai, O.; Wijayanti, K.; Kumar, A.; Kamasamudram, K.; Currier, N. W.; Yezerets, A.; Olsson, L., Comparison of Cu/BEA, Cu/SSZ-13 and Cu/SAPO-34 for ammonia-SCR reactions. *Catalysis Today* **2015,** *258*, 49-55.

67.   Shichi, A.; Satsuma, A.; Hattori, T., Influence of geometry-limited diffusion on the selective catalytic reduction of NO by hydrocarbons over Cu-exchanged zeolite. *Applied Catalysis B: Environmental* **2001,** *30* (1), 25-33.

68.   Wang, A.; Wang, Y.; Walter, E. D.; Washton, N. M.; Guo, Y.; Lu, G.; Peden, C. H. F.; Gao, F., NH3-SCR on Cu, Fe and Cu+Fe exchanged beta and SSZ-13 catalysts: Hydrothermal aging and propylene poisoning effects. *Catalysis Today* **2017**.

69.   Delic, A. Characterization of copper cations in zeolite Y in presence of silver cations; the two-cation effect. NTNU, Trondheim, 2009.

70.   Gao, F.; Walter, E. D.; Washton, N. M.; Szanyi, J.; Peden, C. H. F., Synthesis and Evaluation of Cu-SAPO-34 Catalysts for Ammonia Selective Catalytic Reduction. 1. Aqueous Solution Ion Exchange. *ACS Catalysis* **2013,** *3* (9), 2083-2093.

71.   Weller, M.; Overton, T.; Rourke, J.; Armstrong, F., Physical techniques in inorganic chemistry. In *Inorganic Chemistry*, Oxford University Press: 2014; pp 234-236.

72.   Skoog, D. A.; West, D. M.; Holler, F. J.; Crouch, S. R., Mass spectrometry. In *Fundamentals of analytical chemistry*, Cengage Learning: 2014; pp 808-81.

73.   Man, X. J.; Cheung, C. S.; Ning, Z.; Wei, L.; Huang, Z. H., Influence of engine load and speed on regulated and unregulated emissions of a diesel engine fueled with diesel fuel blended with waste cooking oil biodiesel. *Fuel* **2016,** *180* (Supplement C), 41-49.

74.   Hu, X.; Yang, M.; Fan, D.; Qi, G.; Wang, J.; Wang, J.; Yu, T.; Li, W.; Shen, M., The role of pore diffusion in determining NH3 SCR active sites over Cu/SAPO-34 catalysts. *Journal of Catalysis* **2016,** *341* (Supplement C), 55-61.

75.   Nejar, N.; Illán-Gómez, M. J., Potassium–copper and potassium–cobalt catalysts supported on alumina for simultaneous NOx and soot removal from simulated diesel engine exhaust. *Applied Catalysis B: Environmental* **2007,** *70* (1), 261-268.

10.0 Appendices

Appendix A: Additional XRD results

Appendix B: Additional ICP-MS results

Appendix C: Additional deNO$_x$ results

Appendix D: Complete activity diagram for all samples studied

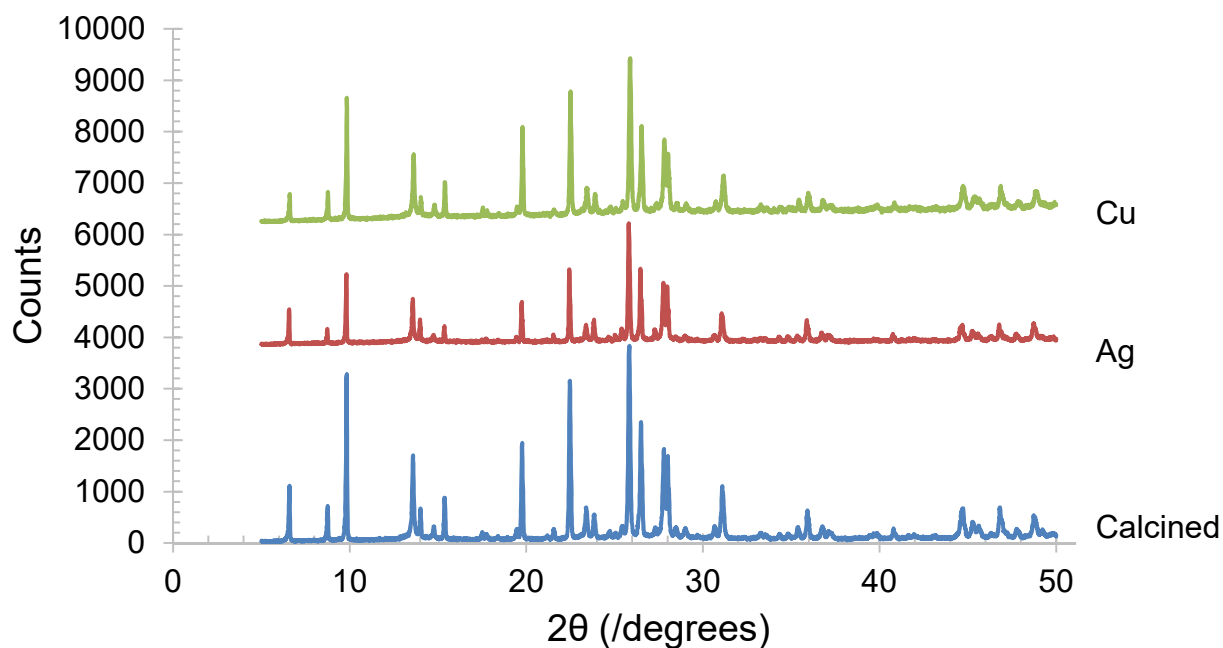# Appendix A: Additional XRD results

Figure A.1: XRD result of first batch of mordenite samples with Ag and Cu. The Ag sample was performed using a different sample holder, and may therefore have different intensity.
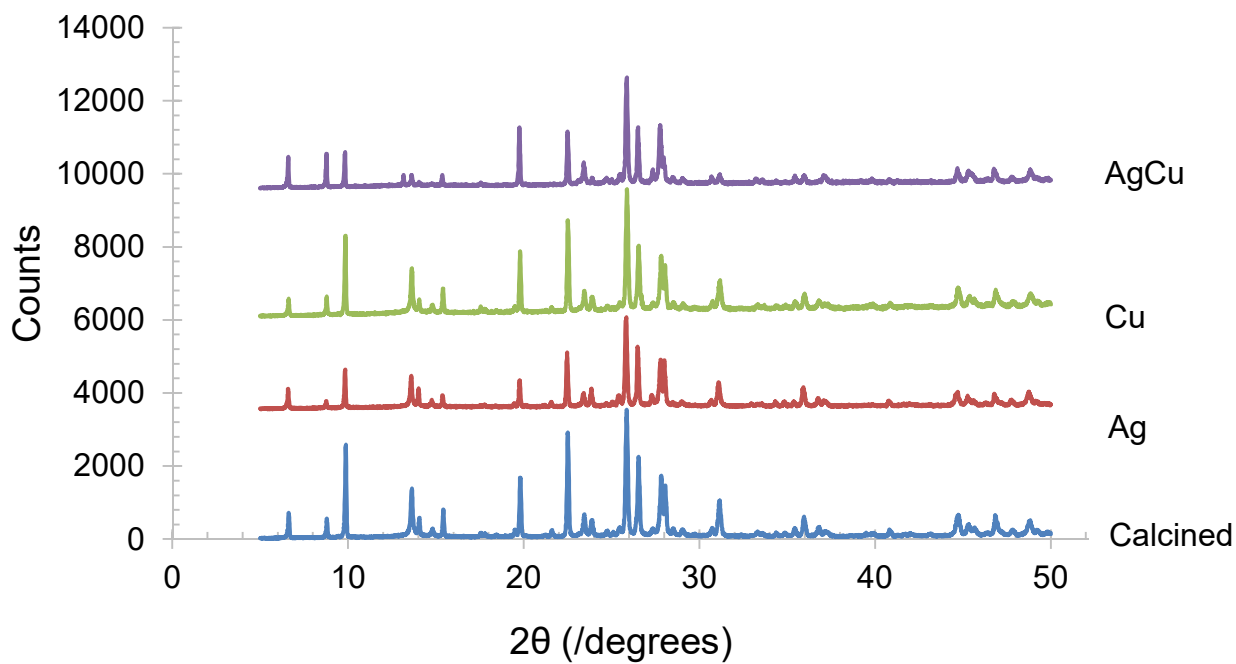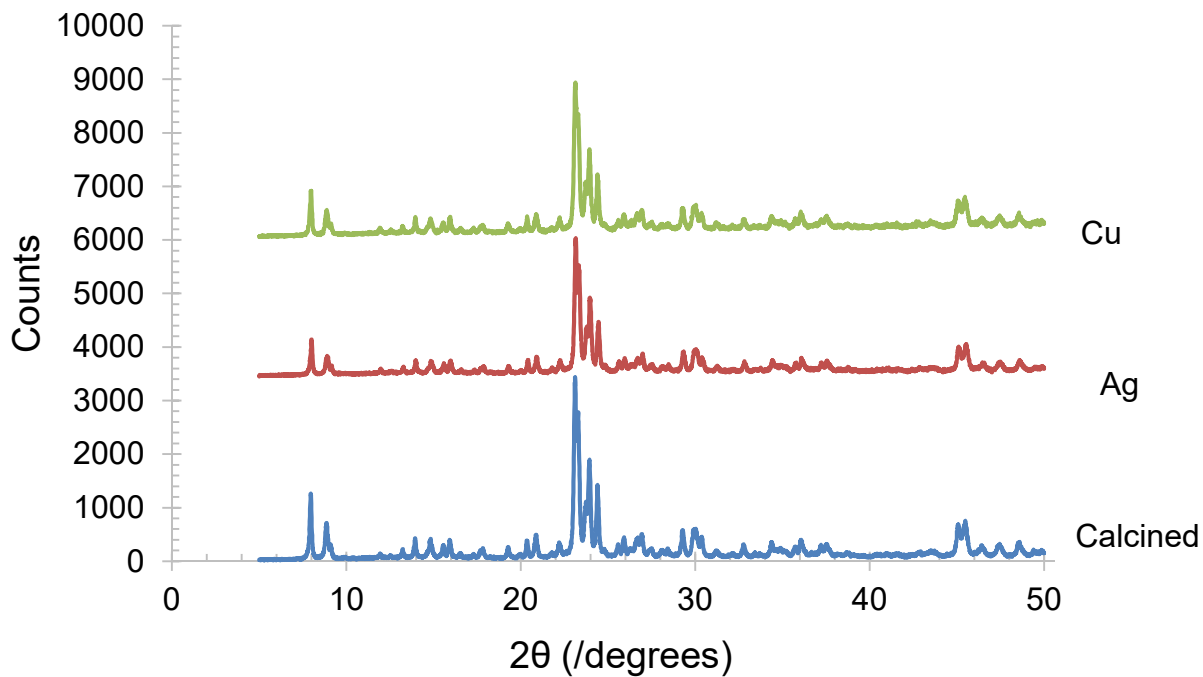

Figure A.2: XRD result of second batch of mordenite samples with Ag and Cu.

Figure A.3: XRD result of first batch of ZSM-5 samples with Ag and Cu.
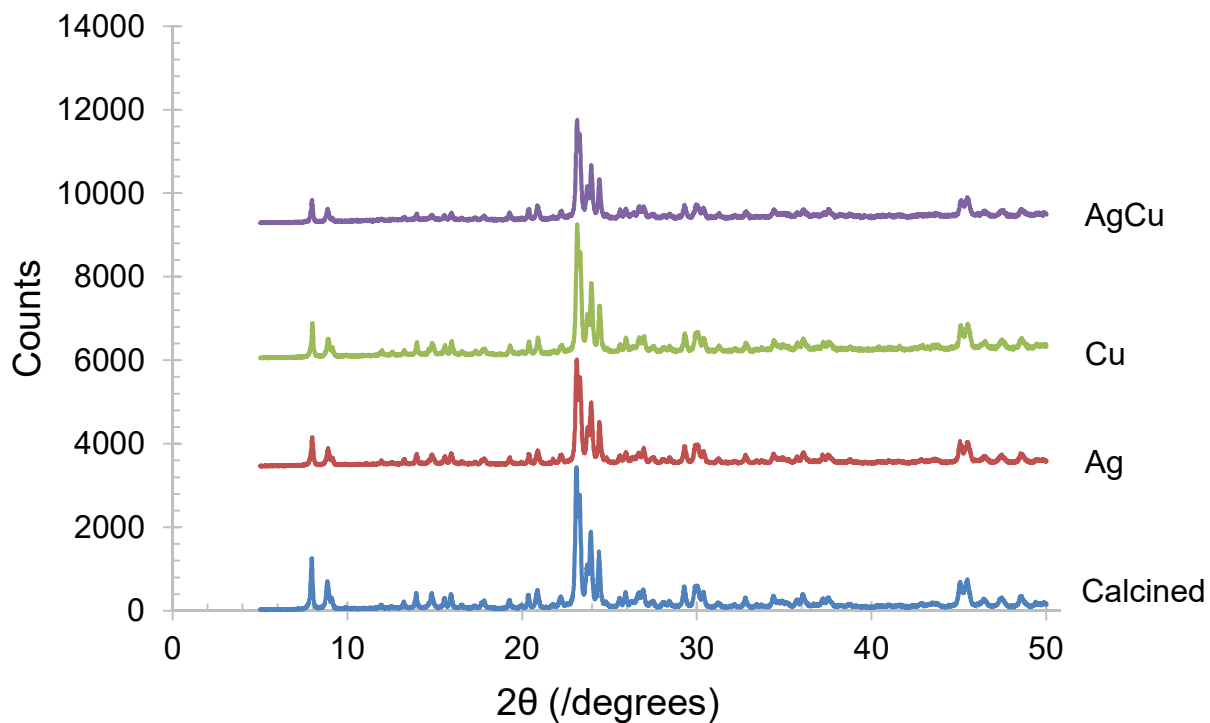
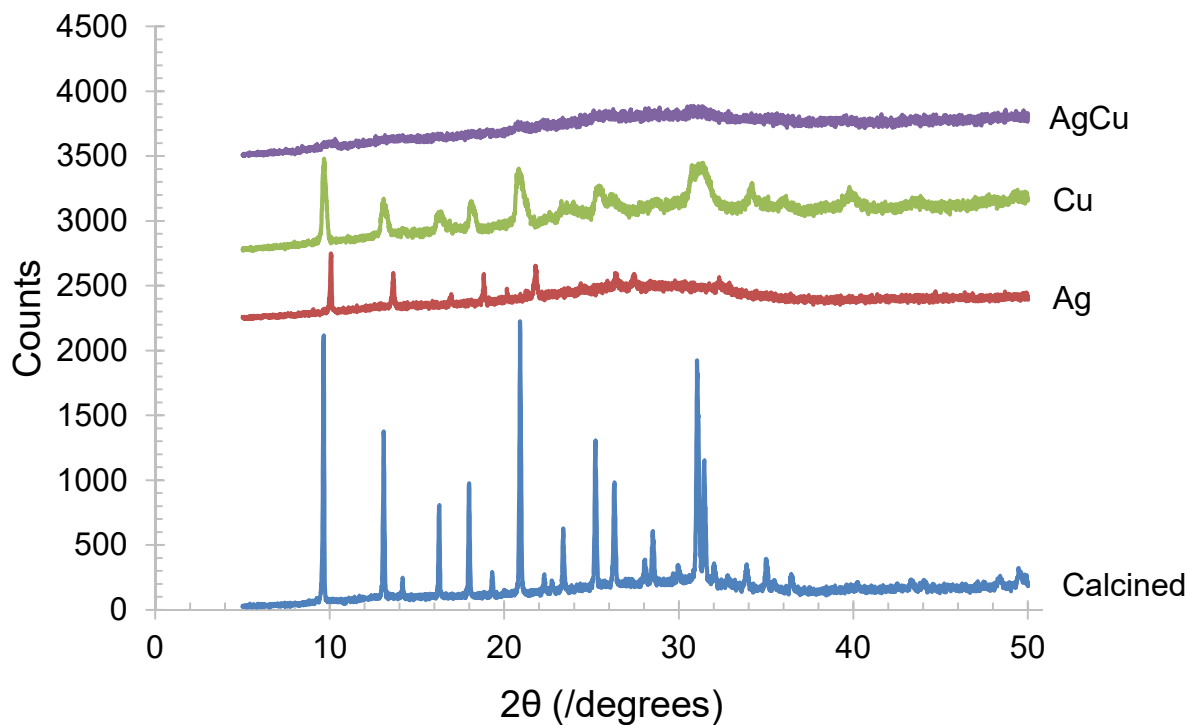*Figure A.4: XRD result of second batch of ZSM-5 samples with Ag and Cu.*

C

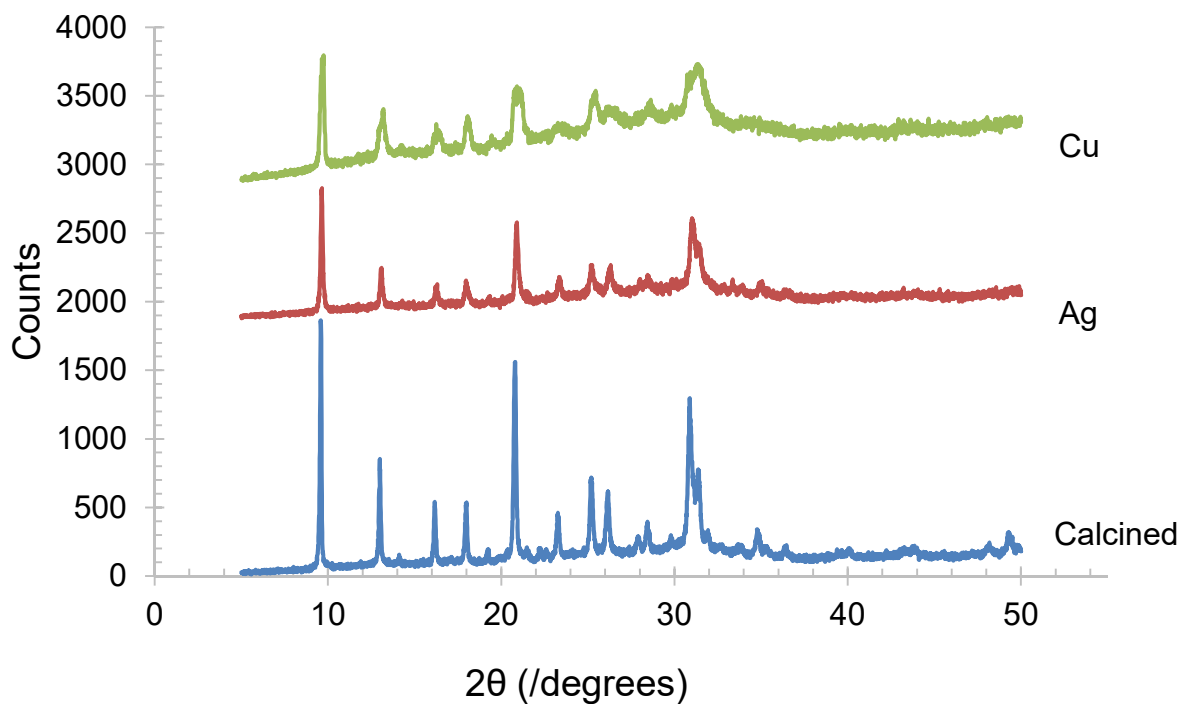*Figure A.5: XRD result of SAPO-34 Hier samples with Ag and Cu.*

Figure A.6: XRD result of first batch of SAPO-34 Conv samples with Ag and Cu. The Cu sample was performed using a different sample holder, and may therefore have different intensity.
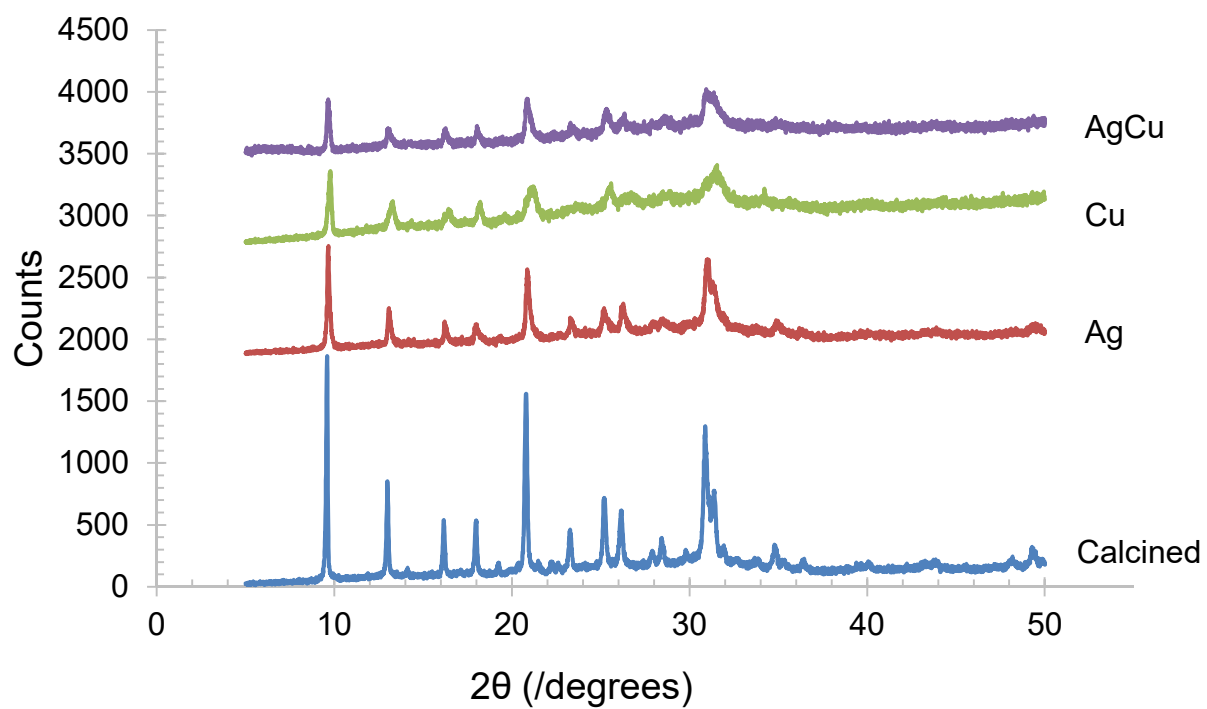
D

Figure A.7: XRD result of second batch of SAPO-34 Conv samples with Ag and Cu.
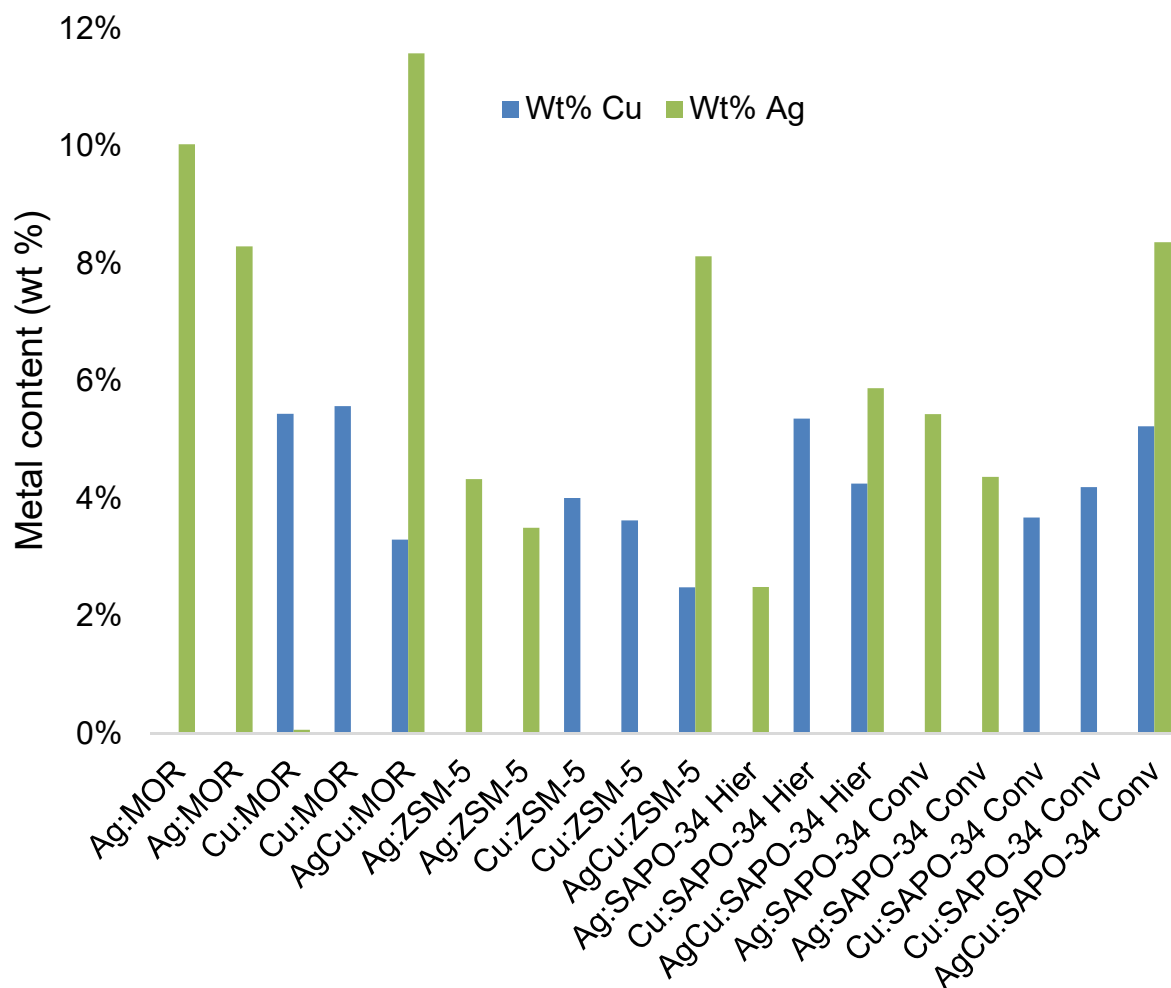
Appendix B: Additional ICP-MS results

Figure B.1: ICP-MS results of all samples used for catalysis.
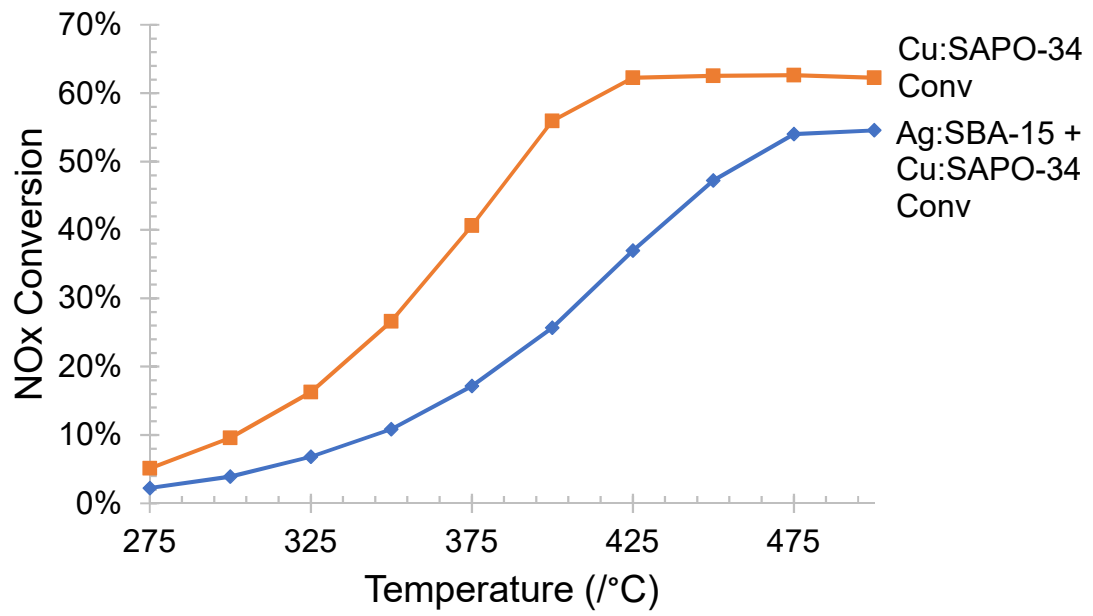
Appendix C: Additional deNOₓ results

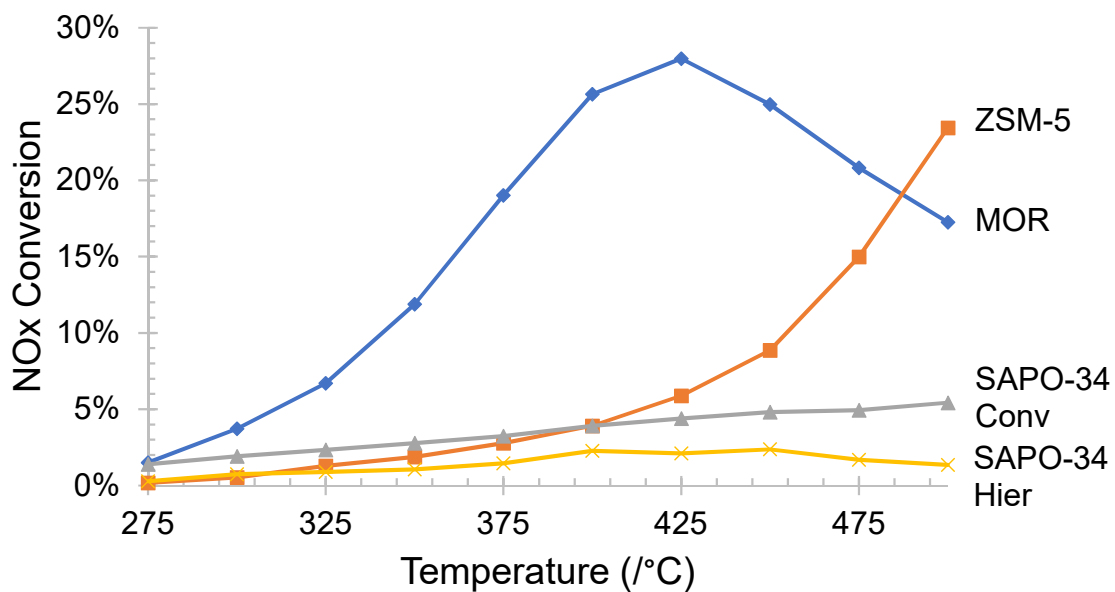*Figure C.1: DeNOₓ results for Ag:SBA-15 + Cu:SAPO-34 Conv and Cu:SAPO-34 Conv.*
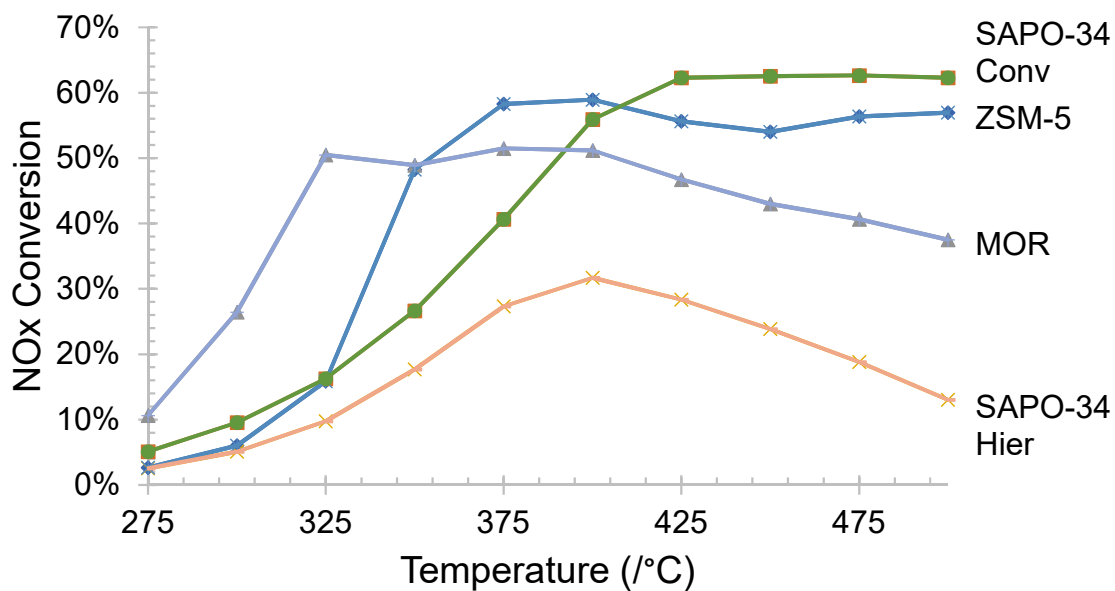
Figure C.2: DeNOx results for Ag:Zeotypes.

Figure C.3: DeNOx results for Cu:Zeotypes.

H

Table D.1: Activity diagram of all samples tested grouped by zeotype.

Zeotype - pore size	275	300	325	350	375	400	425	450	475	500
SAPO-34 Conv - small pore										
Ag										M
Cu									M	
[Ag+Cu]										M
AgCu						M				
ZSM-5 - medium pore										
Ag										M
Cu						M				
[Ag+Cu]										M
AgCu									M	
MOR - large pore										
Ag							M			
Cu					M					
[Ag+Cu]			M							
AgCu				M						
SAPO-34 Hier - mesopore										
Ag								M		
Cu					M					
[Ag+Cu]								M		
AgCu								M		
Mixed Catalysts										
Ag:ZSM-5 + Cu:SAPO-34 Conv										M
Ag:ZSM-5 + Cu:MOR										M
Ag:MOR + Cu:ZSM-5										M
Ag:SBA-15 + Cu:SAPO-34 Conv										M